# Semi-Annual Report

## Nitride Semiconductors for Ultraviolet Detection

Supported under Grant #N00014-92-J-1720
Innovative Science and Technology Office
of the Strategic Defense Initiative
Office of the Chief of Naval Research
Report for the period January 1, 1993–June 30, 1993

Robert F. Davis, K. Shawn Ailey, Bill Perry,
Laura Smith, Cheng Wang,
Warren Weeks and Kim Webber
Materials Science and Engineering Department
North Carolina State University
Campus Box 7907
Raleigh, NC 27695-7907





June 1993





47 pgs

# DISCLAIMER NOTICE

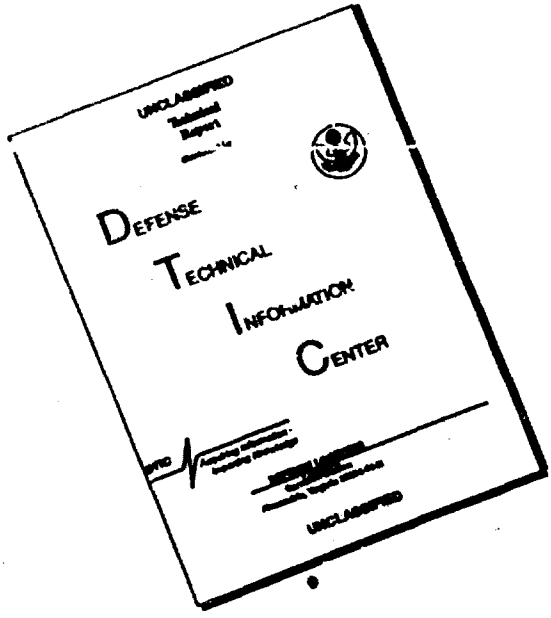


THIS DOCUMENT IS BEST QUALITY AVAILABLE. THE COPY FURNISHED TO DTIC CONTAINED A SIGNIFICANT NUMBER OF PAGES WHICH DO NOT REPRODUCE LEGIBLY.

# REPORT DOCUMENTATION PAGE

*Form Approved*
*OMB No. 0704-0188*



| 1. AGENCY USE ONLY (Leave blank) | 2. REPORT DATE | 3. REPORT TYPE AND DATES COVERED |
|---|---|---|
| | June, 1993 | Semi-Annual 1/1/93–6/30/93 |

**4. TITLE AND SUBTITLE**
Nitride Semiconductors for Ultraviolet Detection

**5. FUNDING NUMBERS**
s400018srr01
1114SS
N00179
N66005
4B855

**6. AUTHOR(S)**
Robert F. Davis

**7. PERFORMING ORGANIZATION NAME(S) AND ADDRESS(ES)**
North Carolina State University
Hillsborough Street
Raleigh, NC 27695

**8. PERFORMING ORGANIZATION REPORT NUMBER**
N00014-92-J-1720

**9. SPONSORING/MONITORING AGENCY NAMES(S) AND ADDRESS(ES)**
Sponsoring: ONR, Code 1513:CMB, 800 N. Quincy, Arlington, VA 22217-5000
Monitoring: Office of Naval Research Resider
The Ohio State University Research Center
1960 Kenny Road
Columbus, OH 43210-1063

**10. SPONSORING/MONITORING AGENCY REPORT NUMBER**

**11. SUPPLEMENTARY NOTES**

**12a. DISTRIBUTION/AVAILABILITY STATEMENT**
Approved for Public Release; Distribution Unlimited

**12b. DISTRIBUTION CODE**

**13. ABSTRACT** *(Maximum 200 words)*

GaN and AlN have been deposited on sapphire and SiC using gas-source MBE and extensively investigated via high resolution TEM. Below the critical thickness, AlN only contains threading dislocations emanating from the misfit dislocations; above this thickness, defects parallel to the growth surface greatly increase. The defect density of AlN grown on SiC at 1100°C is much lower than that contained in material deposited at 700°C. Deposition of GaN on sapphire or SiC results in a larger number of threading dislocations caused by the large misfit as well as a high concentration of dislocations parallel to the growth surface. Both types of defects are decreased in density if the GaN is deposited on AlN. Monocrystalline GaN thin films have also been deposited via layer-by-layer deposition on SiC(0001) substrates from triethylgallium and ammonia. Source concentrations of Ga and exposure times strongly affect the growth process. The near surface region of monocrystalline BP has been converted to BN via exposure to atomic N produced from $N_2$ in an ECR source, as proven by XPS measurements. Current-voltage measurements show an increase in resistance by a factor of 40 after the conversion. Development of (1) ohmic and rectifying contacts, (2) facilities for reactive ion etching and (3) a photo- and cathodo-luminescence system are also underway.

| 14. SUBJECT TERMS | 15. NUMBER OF PAGES |
|---|---|
| thin films, GaN, AlN, gas-source MBE, sapphire, SiC, threading dislocations, layer-by-layer deposition, BP, BN, ohmic and rectifying contacts, reactive ion etching, photoluminescence, cathodoluminescence | 44 |
| | 16. PRICE CODE |

| 17. SECURITY CLASSIFICATION OF REPORT | 18. SECURITY CLASSIFICATION OF THIS PAGE | 19. SECURITY CLASSIFICATION OF ABSTRACT | 20. LIMITATION OF ABSTRACT |
|---|---|---|---|
| UNCLAS | UNCLAS | UNCLAS | SAR |

# Table of Contents

# I. Introduction

Continued development and commercialization of optoelectronic devices, including light-emitting diodes and semiconductor lasers produced from III–V gallium arsenide-based materials, has also generated interest in the much wider bandgap semiconductor mononitride materials containing aluminum, gallium, and indium. The majority of the studies have been conducted on pure gallium nitride thin films having the wurtzite structure, and this emphasis continues to the present day. Recent research has resulted in the fabrication of p–n junctions in wurtzitic gallium nitride, the deposition of cubic gallium nitride, as well as the fabrication of multilayer heterostructures and the formation of thin film solid solutions. Chemical vapor deposition (CVD) has usually been the technique of choice for thin film fabrication. However, more recently these materials have also been deposited by plasma-assisted CVD and reactive and ionized molecular beam epitaxy.

The program objectives in this reporting period have been (1) the investigation of the defects generated during the growth of GaN and AlN on SiC(0001) and sapphire, (2) the layer-by-layer deposition of Ga and N for the growth of GaN films, (3) the conversion of monocrystalline BP to BN via interaction with atomic N from an ECR source and (4) the development of facilities for the deposition of ohmic and rectifying contacts, reactive ion etching and photo- and cathodo-luminescence for III-V materials.

The procedures, results, discussions of these results and conclusions of these studies are summarized in the following sections with reference to appropriate SDIO/ONR reports for details. Note that each major section is self-contained with its own figures, tables and references.

# II. Deposition of GaN PN Junctions and TEM Study of the Structure of AlN and GaN Films Deposited by a Modified Gas Source Molecular Beam Epitaxy System

## A. Introduction

Most recently, the research of GaN PN junction type light emitting diodes (LED) has made significant progress. Several groups have reported that GaN PN junctions have been successfully deposited, and have observed blue light emission [1–4]. However, to date, all reported GaN PN junction LED devices were made by a MOCVD technique. In addition, to exhibit P-type character, Mg-, or Zn-doped GaN films still need post-growth treatment, such as post-deposition Low-Energy Electron-Beam Irradiation (LEEBI) or annealing at high temperatures in a nitrogen environment.

In the last report, we had shown that by a modified gas source molecular beam epitaxy system (GSMBE), we were able to deposit p-type Mg-doped GaN films directly, i.e., without any post-growth treatment. In this report, we will show the further success of the deposition of GaN PN junctions by GSMBE.

Also in this report, we will show microstructural analysis by transmission electron microscopy of our AlN and GaN films deposited under various different growth conditions.

## B. Experimental Procedure

The deposition system employed in this research was a commercial Perkin-Elmer 430 MBE system. This system consists of three parts: a load lock (base pressure of $5*10^{-8}$ Torr), a transfer tube (base pressure of $1*10^{-10}$ Torr), which also was used for degassing the substrates, and the growth chamber (base pressure of $5*10^{-11}$ Torr). Knudson effusion cells with BN crucibles and Ta wire heaters were charged with 7N pure gallium, 6N pure aluminum, 6N pure magnesium and 6N pure silicon respectively. Ultra-high purity nitrogen, further purified by a chemical purifier, was used as the sources gas. The nitrogen gas was excited by an ECR plasma source, which was designed to fit inside the 2.25 inch diameter tube of the source flange cryoshroud. The details of the system can be found elsewhere [5].

The substrates were (0001) oriented $\alpha$(6H)-SiC wafers obtained from Cree Research, Inc. Prior to loading into the chamber, the $\alpha$-SiC substrates were cleaned by a standard degreasing and RCA cleaning procedure. All substrates were then mounted on a 3-inch molybdenum block and loaded into the system. After undergoing a degassing procedure (700°C for 30 minutes), the substrates were transferred into the deposition chamber. Finally RHEED was performed to examine the crystalline quality of the substrates.

C. Results

*Deposition of GaN PN Junctions*. Based on previous research results of the deposition of individual p-type Mg-doped GaN and n-type Si-doped GaN films, we have deposited the GaN PN junctions by a two-step and one-mask process.

We first deposit Si-doped GaN on the substrate. During this step, we initially expose the substrates to pure Al followed by exposure of this Al to the plasma activated nitrogen species in order to form an AlN layer. By this procedure, we have eliminated a thin amorphous layer on the substrate surface due to the plasma exposure. The film growth was subsequently started using the deposition conditions listed in Table I. An AlN buffer layer, having a thickness of about 150Å, was used to reduce the lattice mismatch and was followed by a layer of Si-doped GaN, which was ~3000Å thick.

Table I. Deposition Conditions for Si-doped GaN Films

| | |
|---|---|
| Nitrogen pressure | $2\times10^{-4}$ Torr |
| Microwave power | 50W |
| Gallium cell temperature | 990°C |
| Aluminum cell temperature | 1120°C |
| Silicon cell temperature | 1180°C |
| substrate temperature | 650°C |
| Al layer | 2 monatomic layer |
| AlN buffer layer | 150~200Å |
| Si-doped GaN | 3000~4000Å |

Then the sample was taken out of the system and a mask with defined open area was put on the top of the sample. With this mask we can make electrical contacts on the covered area of n-type Si-doped GaN, since we do not have a GaN etching facility to form the contacts.

Secondly, a layer of Mg-doped GaN (~3000Å thick) was deposited on the masked n-type GaN film by the conditions listed in Table II.

*Characterization of GaN PN Junctions*. Currently, we have only made IV measurements on these GaN PN junctions. The contacts for the measurement were made by two spring probes. IV curves were measured by a Hewlett Packard 4145 Semiconductor Parameter Analyzer. Typical IV curves are shown in Fig. 1 for the GaN PN junction on a sapphire substrate and in Fig. 2 for the GaN PN junction on an α-SiC substrate. The p-type character of the top Mg-doped GaN films was verified by the hot probe method.

Table II. Deposition Conditions for Mg-doped GaN Films

| | |
|---|---|
| Nitrogen pressure | 2*10-4 Torr |
| Microwave power | 50W |
| Gallium cell temperature | 990°C |
| Magnesium cell temperature | ~300°C |
| substrate temperature | 650°C |
| Mg-doped GaN | 3000~4000Å |

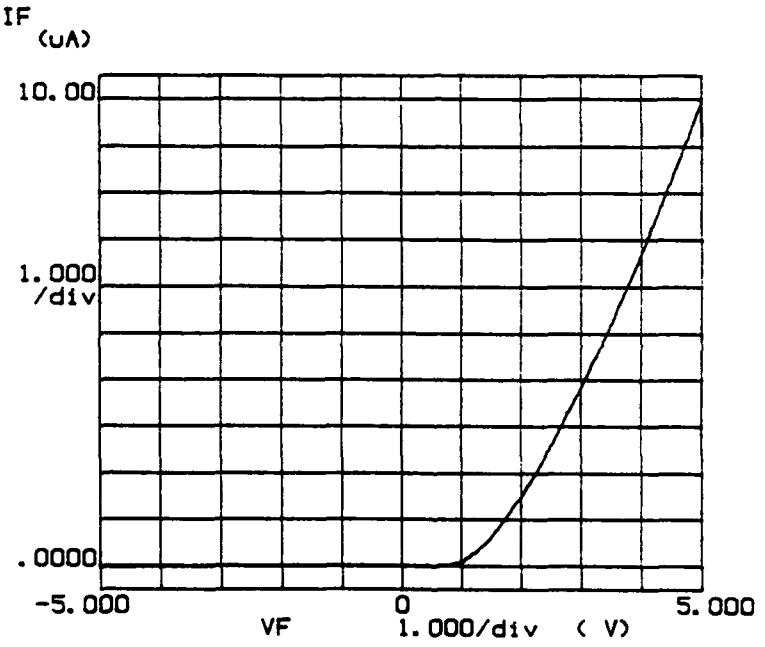


Figure 1. IV curve for the GaN PN junction on (0001) sapphire substrate.

Rectifying characteristics have been observed for the PN GaN junctions on both α-SiC and sapphire substrates. The turn-on voltages for both junctions are about 2 volts. At the same bias, the forward current for the junction on an α-SiC substrate is much larger than the junction on a sapphire substrate.

Further investigation of these junctions is underway, such as ohmic-metal contacts on either n- or p-type GaN layers, reactive ion etching of GaN films in order to deposit n- and p-type GaN layers without interruption, as well as electroluminescence measurements.

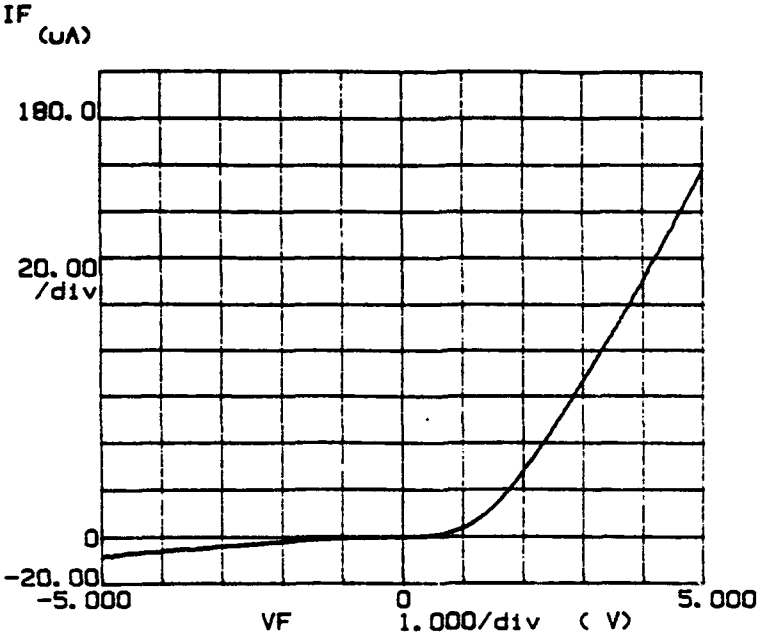


Figure 2. IV curve for the GaN PN junction on (0001) α-SiC substrate.

*Electron Microscopy Characterization of AlN and GaN Films*. The microstructure of the nitride films deposited by GSMBE was characterized by Transmission Electron Microscopy (TEM). The effect of various deposition conditions on the microstructure was investigated.

The TEM was performed in a JEOL 4000EX operated at 400kV. High resolution images were recorded using a 1mr convergence semi-angle at Scherzer defocus (~ -47nm). Cross-sectional transmission electron microscopy (XTEM) samples were prepared using standard techniques.

*TEM Characterization of AlN Films*. Previously, high quality AlN films had been deposited as buffer layers for the growth of GaN films using a modified GSMBE system. High resolution TEM indicated that these films had a highly oriented columnar structure [6]. Here we have investigated any structure change with respect to an increase in film thickness. As shown in Fig. 3, when the film thickness is increased above the critical thickness while maintaining the same deposition conditions, the density of defects which are parallel to the growth surface has greatly increased. The average width of the columnar features is about the same as that seen in the thin, ~100Å, AlN buffer layers. Both AlN films exhibited single crystal RHEED patterns.

The deposition temperature of our AlN films (~650°C) is much lower than what is most commonly used for MOCVD (above 1000°C). To improve the quality of the AlN films, the deposition temperature was raised to 1100°C while keeping other conditions the same. Figure 4

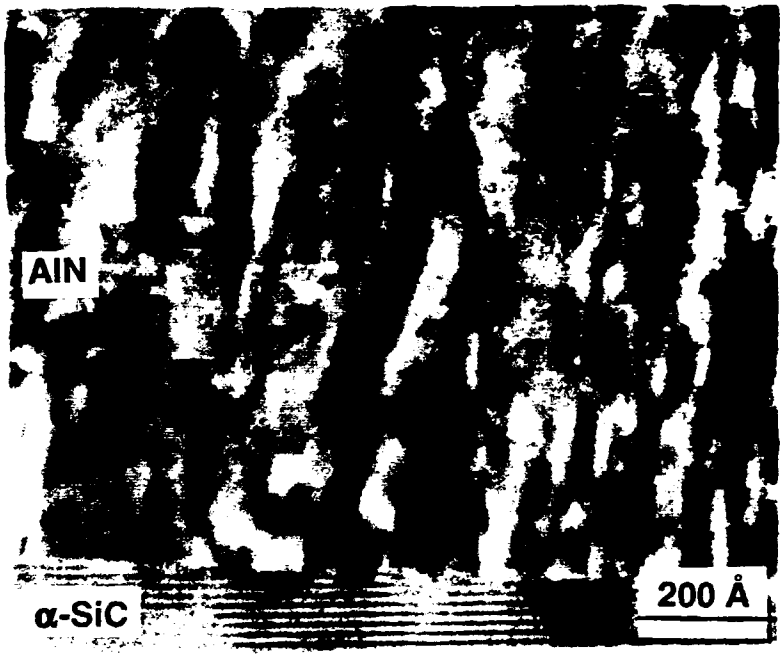


Figure 3. TEM micrograph of an AlN film deposited at 650°C.

is a TEM micrograph of an AlN film deposited at this higher temperature, 1100°C. Defects running perpendicular to the substrate have been greatly reduced, and defects parallel to the growth surface have been removed. A high resolution TEM micrograph of this AlN film, Fig. 5, shows the epitaxial AlN/α-SiC interface.

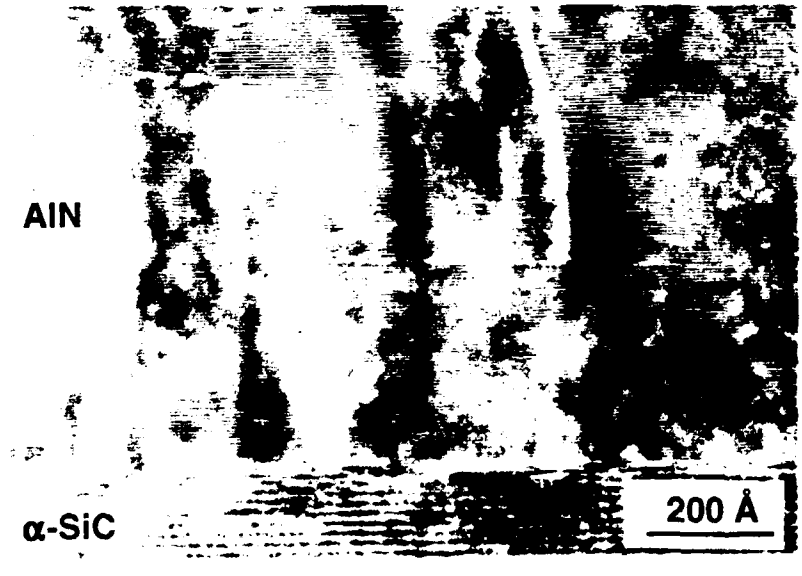


Figure 4. TEM micrograph of an AlN film deposited at 1100°C.

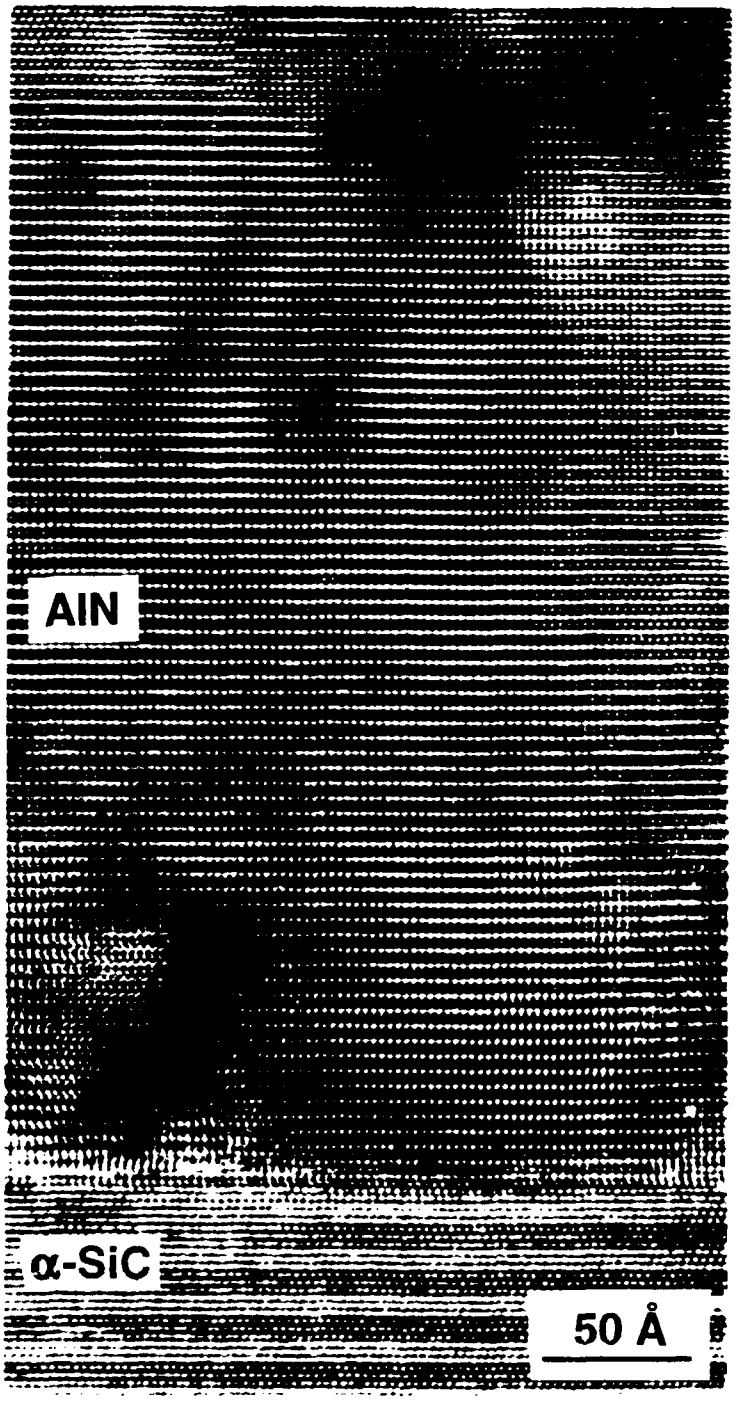


Figure 5. HRTEM micrograph of AlN film deposited at 1100°C.

*TEM Studies of GaN Films*. By a modified gas source molecular beam epitaxy system high quality GaN films have been deposited on both sapphire and α-SiC substrates [6]. RHEED, X-ray diffraction and electron diffraction have indicated that the films are single crystalline. However, as we reported before, TEM revealed that the GaN films still had a columnar

structure. In order to reduce or eliminate these columnar features, we have investigated the effects of various different growth conditions. We limited our study to GaN films deposited on (0001) α-SiC substrates.

The TEM micrographs shown in Fig. 6 are of two GaN films deposited under the same growth conditions except for differing buffer layers. The film shown in Fig. 6 (a) has an AlN buffer layer for which the AlN was deposited at the same temperature as the GaN (650°C), while in Fig. 6 (b), there is no buffer layer. In the film with the buffer layer, there are fewer defects in the GaN close to the AlN buffer layer although increase in number further from the buffer layer. Comparison of Figs. 6 (a) and (b) reveals that the film without the buffer layer has more defects which are parallel to the growth surface and more of a columnar structure than the film with the buffer layer (with respect to the region of GaN close to the buffer layer). Since we know that the growth of high quality, epitaxial AlN films has been achieved at a higher deposition temperature on α-SiC substrates, we have attempted to eliminate the


Figure 6. TEM micrograph of (a) GaN(650°C)/AlN(650°C)/α-SiC

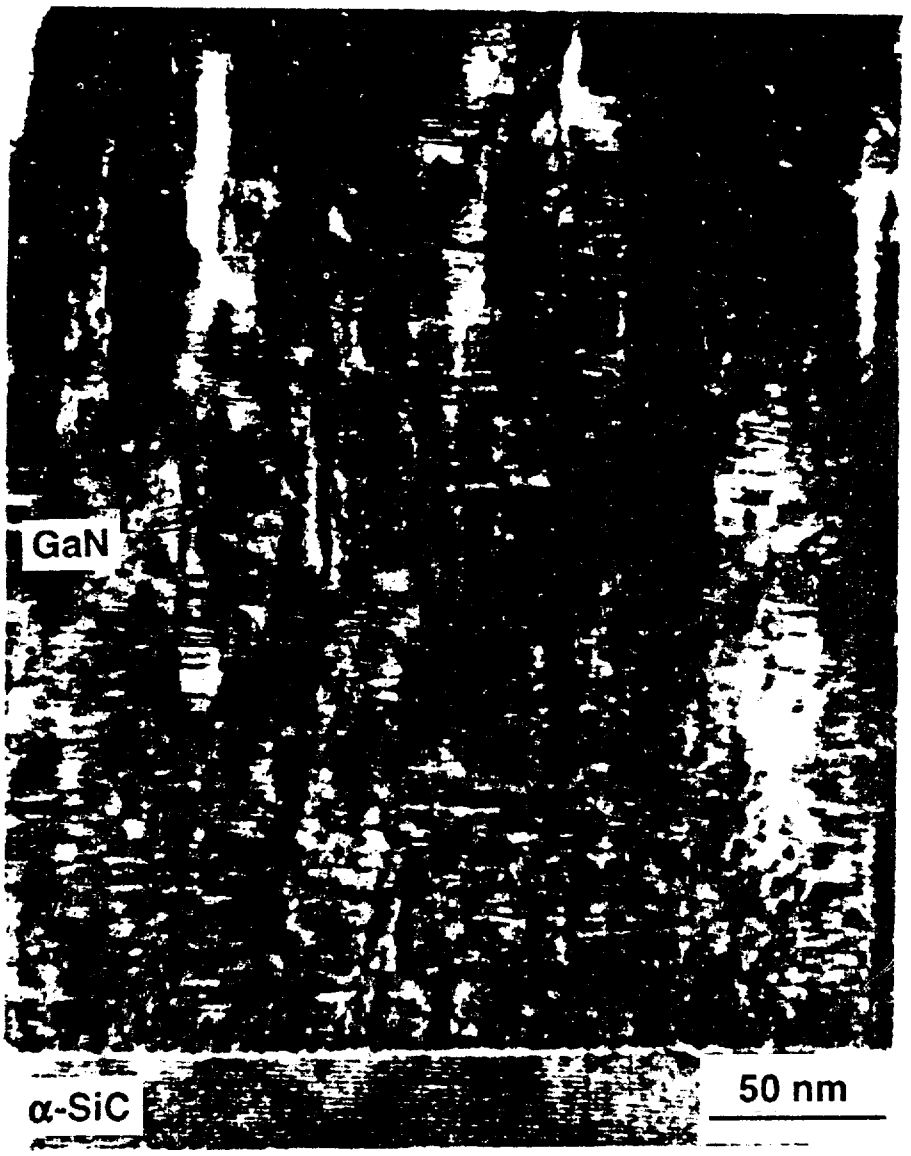


Figure 6. Continued—TEM micrograph of (b) GaN(650°C)/α-SiC.

columnar structure by depositing the AlN buffer layer at 1100°C proceeded by the deposition of GaN at 650°C on this AlN layer. Scanning electron microscopy showed very fine surface features, however, XTEM revealed that the film again consisted of a columnar structure, as shown in Fig. 7. No apparent improvement was gained from the increase in deposition temperature of the AlN layer.

Figure 8 is a TEM micrograph of a GaN film deposited at a reduced deposition rate (five times less) and longer deposition time than the GaN film shown in Fig. 7. Again there was no apparent improvement. Furthermore, the columnar features of the film in Fig. 8 increased in number as the growth proceeded. This is similar to what was observed in the film shown in Fig. 6(a).


Figure 7. TEM micrograph of GaN(650°C)/AlN(1100°C)/α-SiC.

D. Discussion

There have been a lot of reports recently on the deposition of high quality single crystal GaN films [2,4,7–9]. There are two key factors realized by most MOCVD research groups, that is: i) the need for low temperature deposition of AlN or GaN buffer layers with a thickness of about 300~500Å; ii) the thickness of the GaN films needs to be 3mm or more. To date, no clear microstructural images have been presented of these high quality single crystal GaN films, especially those revealing the change in film structure with the different film thicknesses. However, several TEM pictures of the buffer layer or GaN layer near the substrate interface have been reported [9,10]. In the above section, we have presented TEM results for our GaN films deposited at various growth conditions.

In summary, we have realized that, like MOCVD, the GaN films with the buffer layer are better than the GaN films without the buffer layer. It is has been generally accepted that the buffer layer is either for stress relief or for reduction of the lattice mismatch between the


Figure 8. TEM micrograph of GaN(650°C)/AlN(1100°C)/α-SiC, the deposition rate for the GaN film was five time less than the rate for the GaN film in Figure 5.

substrate and the GaN film; the lattice mismatch between AlN/α-SiC or AlN/sapphire is less than that between GaN/α-SiC or GaN/sapphire, respectively. However, even though AlN has been used as a buffer layer between GaN and the substrate, there is still a 2.4% lattice mismatch at the GaN/AlN interface. The columnar features we have observed in the GaN films may result from the lattice mismatch. As the GaN film becomes thicker, the stress due to lattice mismatch builds up, and the columnar features become more significant. This is quite different from what MOCVD results indicate. That is, single crystal GaN film growth can be accomplished only when the films were 3mm or more in thickness.

To obtain very high quality GaN films, the columnar structure must be eliminated throughout the films. The deposition temperatures of GaN by GSMBE were much lower than

what has been used in MOCVD. However, in the low pressure deposition process of GSMBE, the deposition temperature is really limited by the desorption rate of GaN [11]. As we have shown before, when the growth temperature was increased to 900°C almost no GaN film was deposited. Therefore, we have to pursue another way to overcome the columnar structures in the films if we cannot increase the deposition rate of the GaN films dramatically by GSMBE.

As we indicated before, the lattice mismatch still exists even when epitaxial AlN was used as a buffer layer between GaN and the α-SiC substrate. In contrast to MOCVD, in which the AlN buffer layer can be amorphous or polycrystalline, we cannot deposit epitaxial GaN films by GSMBE unless the AlN buffer layer is of good crystal quality. Therefore the 2.4% lattice mismatch between AlN and GaN may play an important role in the columnar features in the GaN film. A direct way to reduce this lattice mismatch is to deposit an epitaxial buffer layer consisting of an AlN layer slowly graded to GaN on the substrate followed by the deposition of a GaN film on this graded buffer layer. However, as we found in our preliminary study, there was an abrupt change from an AlN-rich layer to a GaN-rich layer instead of a gradual graded layer. This is possibly due to the stronger attraction of Al to N than the attraction of Ga to N. Therefore, further research needs to be carried out to improve the deposition of a real graded layer.

## F. Future Research Plans

As noted in the discussion part of this report, due to the limitation of GSMBE a graded $Al_xGa_{1-x}N$ solid solution buffer layer, from x=1 to x=0, would be an ideal solution for the homoepitaxy growth of GaN. Some of our future efforts will continue to involve the growth of good quality graded $Al_xGa_{1-x}N$ solid solution buffer layers. Also, we will continue our efforts to make GaN PN junction LED devices, and to study ohmic metal contacts on GaN films, reactive etching of GaN to define device structure and electroluminescence of GaN PN junction LEDs.

## G. References


1. B. Goldenberg, J. D. Zook and R. J. Ulmer, Appl. Phys. Lett. **62**, 381 (1993).
2. I. Akasaki, H. Amano, N. Koide, M. Kotaki and K. Manabe, Physic B **185**, 428 (1993).
3. M. R. H. Khan, I. Akasaki, H. Amano, N. Okazaki and K. Manabe, Physic B **185**, 480 (1993).
4. S. Nakamura, M. Senoh and T. Mukai, Jpn J. Appl. Phys. **32**, L9 (1993).
5. Z. Sitar, M. J. Paisley, D. K. Smith and R. F. Davis, Rev. Sci. Instrum. **61**, 2407 (1990).
6. R. F. Davis *et al.*, R. F. Davis *et al.*, in Final Technical Report N00014-90-J-1427, P34–35 (1992).
7. M. A. Khan, J. N. Kuznia, D. T. Olson, R. Kaplan, J. Appl. Phys. **73**, 3108 (1993).
8. I. Akasaki, H. Amano, M. Sassa, H. Kato and K. Manabe, J. Crystal Growth **128**, 379 (1993).

9. J. N. Kuznia, M. A. Khan, D. T. Olson, R. Kaplan and J. Freitas, J. Appl. Phys. **73**, 4700 (1993).
10. N. Kuwano, T. Shraishi, A. Koga, K. Oki, K. Hiramatsu, H. Amano, K. Itoh and I, Akasaki, J. Crystal Growth **115**, 381 (1991).
11. N. Newman, J. Ross, and M. Rubin, Appl. Phys. Lett. **62**, 1242 (1993).

# III. Layer-by-layer Deposition of III-V Nitrides Using an Atomic Layer Epitaxy Reactor Design

## A. Introduction

The potential semiconductor and optoelectronic applications of III-V nitrides has prompted significant research in thin film growth and development. The materials of concern in this section are GaN, currently, and other III-V nitrides, for upcoming studies. Because GaN in the wurtzite structure with a bandgap of 3.4 eV [1] forms continuous solid solutions with both AlN and InN, for example, which have bandgaps of 6.2 eV [2] and 1.9 eV [3], respectively, engineered bandgap materials could result in optoelectronic devices active from the visible to deep UV frequencies [4].

Initial attempts at ALE deposition have been suspended in favor of the more realistic layer-by-layer deposition approach. This decision was supported by metalorganic decomposition data and by actual experimentations completed thus far. Like ALE, the layer-by-layer technique deposits one monolayer of material per cycle. However, the growth rate is highly dependent on the metalorganic (MO) flux and the exposure time under the MO gas. Thus unlike ALE, the process is not self-terminating after the deposition of one monolayer.

To produce films using the layer-by-layer approach an ALE reactor design has been implemented. The equipment and experimental procedures used for the process have been discussed in an earlier report. Therefore, only modifications to the experimental procedure, new results to date, conclusions and plans for future work will be included here.

## B. Experimental Procedure

The ALE reactor design being used utilizes a continuously rotating susceptor arrangement. Thus as the susceptor rotates, the substrate is alternately exposed to the me MO gas, the $H_2$ curtain gas and the nitrogen source gas (i.e. ammonia: $NH_3$) in a constant cycle. There are two growth zones per cycle: one for the column-III species and one for the column-V species. For layer-by-layer growth, one cycle will result in one monolayer of film growth.

Unlike earlier work in which rotation began from under the $H_2$ inlet line before the MO inlet line, recent experiments have begun with initial exposure to ammonia. Before the substrate sweeps under the ammonia inlet line, the W-filament used in cracking the ammonia into elemental hydrogen and nitrogen should be stabilized at the desired "cracking" temperature. The nitrogen source was chosen as the starting species because it was believed that initial exposure to the MO precursor was possibly aiding in the faceted growth being observed by not uniformly covering the substrate surface. It was believed that more uniform coverage would result from this and instigate the desired uniform growth. This step will be termed "nitrogenating" the substrate surface. Thus, prior to the exposure to any TEG, the substrate

was nitrogenated for 5 seconds at the start of the run. Similarly, at the end of the run the deposited film was nitrogenated for 5 seconds after the flow of TEG had been terminated.

Also in an attempt to reduce the faceted surfaces of the deposited films, the growth temperature was lowered from 640°C used in earlier runs to 500°C. By reducing the temperature, the surface mobility is reduced. Hopefully this reduction would result in a more uniform deposition and less atomic migration to the more preferred nucleation sites resulting in the undesired faceted growth.

Once rotation and deposition begins, several system variables must be monitored. They include cooling water flow, all gas flow rates, system and MO bubbler pressures, susceptor and W-filament temperatures, and rotation speed. Under normal operating procedures, these variables remain nearly constant, but because of their obvious importance, they must be monitored to maintain deposition uniformity. Table I below lists the system parameters for various deposition runs.

Table I. Deposition Parameters

| System Variables | Run # #10 | #13 | #14 | #15 | #16 |
|---|---|---|---|---|---|
| Substrate | Si C* | Si C** | Si C** | SiC ** | SiC ** |
| Initial Press. | $1\times10^{-5}$ torr | $1.2\times10^{-5}$ | $1.2\times10^{-5}$ | $1.2\times10^{-5}$ | $1.8\times10^{-5}$ |
| Run Pressure | 3.6-3.8 torr | 2.8-3.0 | 2.9-3.1 | 2.9-3.4 | 2.8-3.0 |
| Bubbler Temp. | 5.0°F | 56.3 | 56.3 | 56.3 | 56.3 |
| Bubbler Press. | ~ 800 torr | ~ 750 | ~ 750 | ~ 750 | ~750 |
| TEG Part. Press. | 0.414 torr | 2.96 | 2.96 | 2.96 | 2.96 |
| $H_2$ flow | ~ 325 sccm | ~ 325 | ~ 325 | ~ 325 | ~ 325 |
| $NH_3$ flow | 100 sccm | 100 | 100 | 200 | 200 |
| $H_2$ carrier gas flow | 28 sccm | 28 | 28 | 28 | 28 |
| TEG flow rate | 0.0145 sccm | 0.111 | 0.111 | 0.111 | 0.111 |
| W-filament Temp. | 1450°C | 1450 | 1450 | 1450 | 1450 |
| Susceptor Temp. | 500°C | 500 | 500 | 500 | ~640 |
| Rotation Speed | 1.6 rpm | 3 | 8.25 | 8.25 | 8.25 |
| Sec/zone | 13.125 | 7 | 2.545 | 2.545 | 2.545 |
| Run Time | 180 minutes | 200 | 140 | 140 | 140 |

* α(6H)-SiC (0001) on axis

** α(6H)-SiC (0001) 3° off-axis toward [11$\bar{2}$0]

C. Results

Run #10 was the first attempt at the 500°C growth temperature. Scanning Electron Microscopy (SEM) images revealed a surface which appeared extremely smooth with no visible facets. However, the growth rate was very slow at this reduced temperature and TEG flow rate. The film was less than a 100Å thick as evident from Auger Electron Spectroscopy (AES). Increasing the TEG flow rate from 0.0145 sccm to 0.13 sccm in the next run in an effort to increase the growth rate yielded a polycrystalline film as indicated by visible rings in the reflected high energy electron diffraction (RHEED) pattern. Slightly decreasing the TEG flow rate to 0.111 sccm and increasing the rotation speed to 3 rpm (7 sec/zone) for Run #13 yielded better results. The RHEED patterns for this film (Figs. 1 & 2) appear monocrystalline.

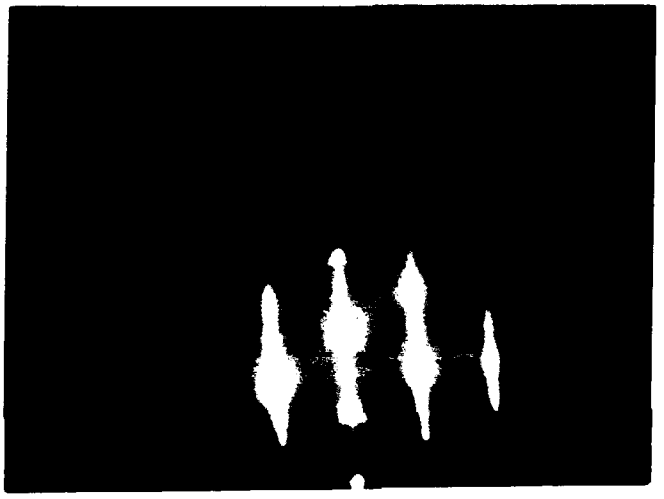

$\{11\bar{2}0\}$ Reflection

Figure 1. RHEED pattern for Run #13 of GaN deposited on α(6H)-SiC at 500°C.

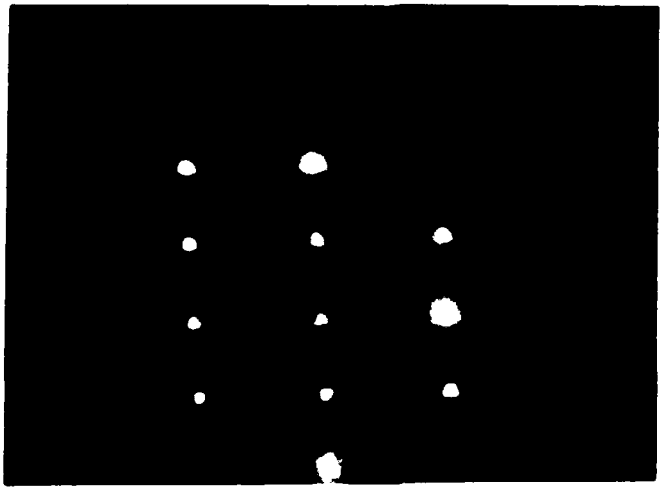

$\{10\bar{1}0\}$ Reflection

Figure 2. RHEED pattern for Run #13 of GaN deposited on α(6H)-SiC at 500°C.

However the diffraction spots are not extremely sharp, a result of the faceted surface. From measurements taken from SEM images, the facets had an approximate average diameter of 500Å. Also, as shown in the graph in Fig. 3 the growth was greater layer-by-layer. Fortunately, results show that at 500°C and a TEG flow rate of 0.111 sccm film deposition is constant at approximately 0.5 Å/sec. Thus by increasing the rotation speed and hence reducing exposure time per zone, layer-by-layer growth was achieved in Run #14 and repeated in Run #15 (Fig. 3). Transmission Electron Microscopy (TEM) on Run #14 revealed apparent columnar growth. SEM of Run #15 revealed a uniformly deposited film but also a faceted surface (Fig. 4). The approximate average facet diameter was 400Å for both Runs #14 and #15, slightly less than the facet size of Run #13. Doubling the flow rate of $NH_3$ from 100 sccm to 200 sccm from Run #14 to #15 caused no readily apparent improvements in film quality. Increasing the growth temperature to 640°C for Run #16 with all other parameters unchanged from Run #15 increased the deposition rate and caused a deviation from layer-by-layer growth. The average facet size of Run #16 as evident from SEM was 1200Å.

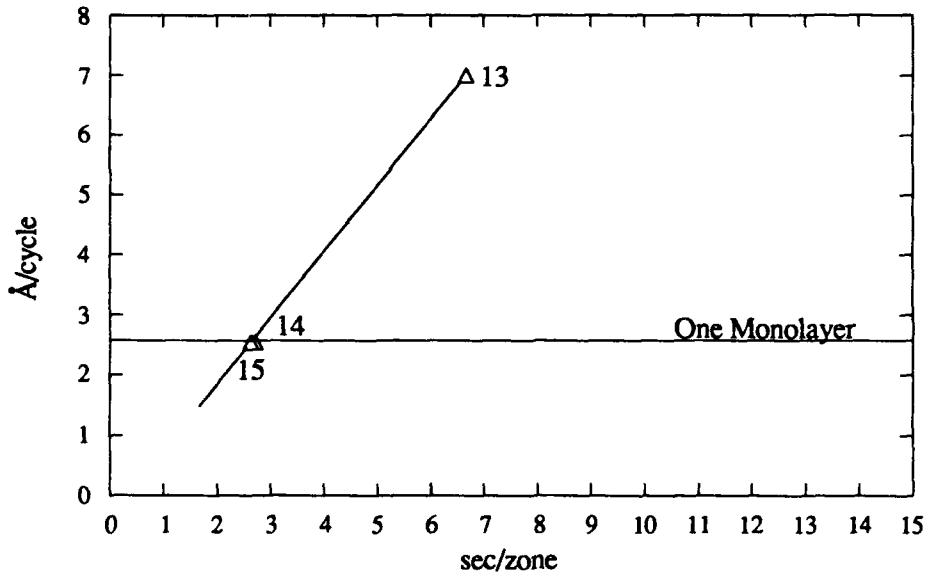


Figure 3. Deposition thickness of GaN per cycle *vs.* exposure time for Run #'s 13, 14 and 15. The growth temperature was 500°C and at a TEG flow rate of 0.111 sccm for each run.

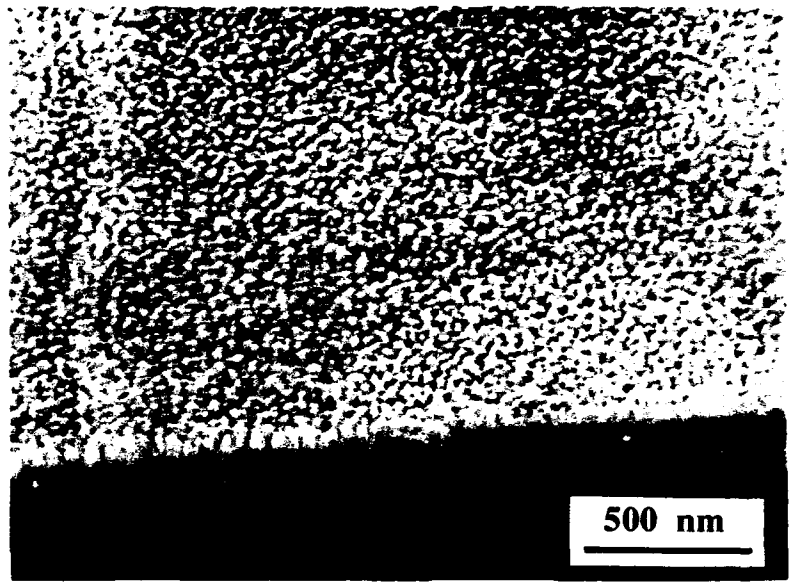


Figure 4. SEM micrograph for Run #15. Notice the uniformly faceted surface. Film thickness is ~3000Å and average facet size is ~400Å.

D. Discussion

*ALE Suspension.* In principle, for ALE growth to occur using metalorganic precursors as the column-III source, the MO gas must adsorb to the substrate in a self-terminating mode. For this reason the decomposition mechanisms of the MO precursors are of obvious importance for determining the viability of ALE. The following organometallics are used as source gases for GaN, AlN and InN respectively: triethylgallium (TEG) [$Ga(C_2H_5)_3$], triethylaluminum (TEA) [$Al(C_2H_5)_3$] and trimethylindium (TMI) [$In(CH_3)_3$].

Various experimental techniques have been used to study the decomposition mechanisms of these MO gases [5–16], with mass spectrometry and thermal desorption being the most prevalent. TE(G,A) consist of the metallic species surrounded by three ethyl ($C_2H_5^+$) functional groups. Each species adsorbs as a monomer [6]. Via mass spectrometry results for the decomposition of TEG with $H_2$ as the carrier gas, the decomposition temperature range was 220°–330°C, with ethylene ($C_2H_4$) being produced [7–9]. This indicates that β-elimination is the dominant decomposition mechanism [5–7,9]. It is also interesting to note that the decomposition temperature range slightly increases (270°-380°C) when $N_2$ is used as the carrier gas [7]. (The decrease in the decomposition temperature contributed to the presence of $H_2$ carrier gas is not fully understood at present.) During β-elimination, one of the hydrogen atoms breaks its bond with the β-carbon and joins to the remaining Ga species to satisfy the charge balance. The hydrocarbon functional group re-orients itself becoming ethylene with a total of four H atoms attached to two double bonded C atoms (Fig. 5).

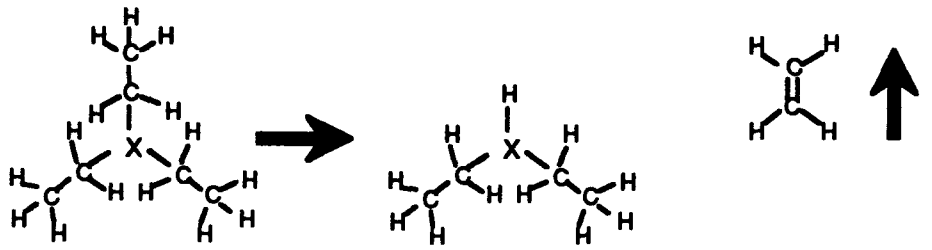

Figure 5. Schematic of the TE(G,A) gas phase decomposition showing β-elimination and the production of ethylene. X represents the column-III species.

Similarly, TEA decomposes by the same β-elimination process at apparently slightly lower temperatures [10]. And presumably to achieve, for example ALE of GaN using TEG, the MO source should only decompose to a diethyl (DEG) or possibly a monoethyl (MEG) species in order for chemisorption to be self-limiting.

TE(G,A) was chosen over TM(G,A) because of its lower decomposition temperature range and a lower carbon incorporation in the growing film during surface decomposition reactions [4]. However, for InN deposition TMI is the organometallic of choice. This results because the TEI precursor is much less thermally stable than its methyl counterpart and undergoes appreciable decomposition starting at 40°C [11] as compared to 270-300°C for TMI [12–15]. However, as expected TMI undergoes a dissimilar decomposition process than that of the triethyl species. As determined by Jacko and Price, TMI predominantly decomposes by homolytic fission and at the low pressures and high temperatures used in many growth techniques methane ($CH_4$) appears to be the principle reaction product [16].

Therefore, due to the relatively low temperatures necessary for the decompositions of TEG, TEA and TMI, the self-terminating growth mechanism required for ALE deposition appears improbable at the increased growth temperatures of interest. Film deposition in the temperature ranges needed for only the partial decomposition of the MO precursors necessary for self-limiting adsorption have yielded only amorphous and polycrystalline films [4]. Hence, ALE deposition has been suspended in favor of the more realistic layer-by-layer approach.

*Experimentations*. From experimentations the growth rate at 500°C and a TEG flow rate of 0.111 sccm is constant at approximately 0.5 Å/sec. Simply by adjusting the susceptor rotation speed and thus the exposure time layer-by-layer deposition was achieved. A constant deposition rate has not been evident at 640°C. This phenomenon can be explained as follows [17]. During the growth period in the TEG zone, TEG molecules adsorb on the surface and decompose into Ga atoms. Additional TEG molecules attached to the Ga adsorbed surface may either decompose into more Ga atoms or desorb from the surface before decomposing. At lower growth temperatures it appears that desorption of the TEG molecules is more dominant than further TEG decomposition. However, as the growth temperature increases, the additional

TEG molecules adsorbed onto the surface decompose more easily into Ga atoms rather than desorb from the surface. This finding is supported by the increased deposition rate between Run #15 and Run #16, grown at 500°C and 640°C, respectively, with all other parameters the same.

## E. Conclusions

Apparent monocrystalline GaN films have been grown using a layer-by-layer deposition technique. After studying the different decomposition mechanisms of the various MO precursors, ALE was suspended in favor of the layer-by-layer approach. Earlier experimentations support this decision.

At a growth temperature of 500°C and a TEG flow rate of 0.111 sccm the deposition rate is constant at approximately 0.5Å/sec. A constant growth rate does not exist at 640°C. This phenomenon was explained by the adsorption-decomposition model described above.

## F. Future Research Plans and Goals

Deposition of GaN using GaN and AlN buffer layers will be attempted. The use of a buffer layer may reduce the effects of lattice mismatch between the SiC substrate and the depositing film and aid in the growth of more desirable, non-faceted films. Additional plots of thickness per cycle versus exposure time need to be established to investigate the layer-by-layer process at differing temperatures and MO precursor flow rates.

Layer-by-layer growth of AlN and InN is upcoming. Electrical measurements such as mobilities and carrier concentrations need to be established for the deposited III-V films. Also, attempts may be made to p-type dope GaN. A grand goal would be layered III-V nitride films and continuous solid solutions.

## G. References


1. H. P. Maruska and J. J. Tietjen, Appl. Phys. Lett. **15**, 327 (1969).
2. W. M. Yim, E. J. Stofko, P. J. Zanzucchi, J. I. Pankove, M. Ettenberg and S. L. Gilbert, J. Appl. Phys. **44**, 292 (1973).
3. J. A. Sajurjo, E. Lopez-Cruz, P.Vogh and M.Cardona, Phys. Rev. **B28**, 4579 (1983).
4. J. Sumakeris, Z. Sitar, K. S. Ailey-Trent, K. L. More and R. F. Davis, Thin Solid Films **225**, 244 (1993).
5. A. J. Murrell, A. T. S. Wee, D. H. Fairbrother, N. K. Singh, J. S. Foord, G. J. Davies and D. A. Andrews, Vacuum, **41(4-6)**, 955 (1990).
6. T. R. Gow, F. Lee, A. L. Backman and R. I. Masel, Vacuum **41(4-6)**, 951 (1990).
7. M. Yoshida, H. Watanabe and F. Uesugi, J. Electrochem. Soc. **132(3)**, 677 (1985).
8. M. Hoshino, J. Crystal Growth, **110** (1991) 704.
9. W. Lee, T. R. Omstead, D. R. McKenna and K. F. Jensen, J. Crystal Growth, **85**, 165 (1987).
10. W. L. Smith and T. Wartik, J. Inorg. Nucl. Chem. **29**, 629 (1967).
11. *CVD Metalorganics for Vapor Phase Epitaxy: Product Guide and Literature Review II*, Advanced Materials, Morton International, Danvers, MA.
12. D. A. Jackson, Jr., J. Crystal Growth **94**, 459 (1989).

13. R. Karlicek, J. A. Long and V. M Donnelly, J. Crystal Growth **68**, 123 (1984).
14. C. A. Larsen and G. B. Stringfellow, J. Crystal Growth **75**, 247 (1986).
15. N. I. Buchan, C. A. Larsen and G. B. Stringfellow, J. Crystal Growth **92**, 591 (1988).
16. M. J. Jacko and S. J. W. Price, Can. J. Chem. **42**, 1198 (1964).
17. N. Kobayashi, T. Makimoto and Y. Horikoshi, Jpn. J. of Appl. Phys. **24**, L962 (1985).

# IV. Converting Boron Phosphoride to Boron Nitride by Exposing to an ECR Nitrogen Plasma

## A. Introduction

Cubic boron nitride (cBN) has significant potential for electronic device applications because it is a wide bandgap semiconductor with very high thermal conductivity. However, the epitaxial growth of single crystal cBN film is found to be extremely difficult due to the thermodynamic instability, the high surface energy and the lack of lattice matched substrate material.

It is known that cubic boron monophosphide (BP) can be epitaxially grown on Si substrates [1–5]. Boron phosphide has an identical structure as cBN. If the top surface layer of phosphorous can be replaced by nitrogen, then the surface structure of BP will be converted to cBN. In this report a preliminary study of converting the surface of a BP film to cBN has been conducted by exposing the BP film to an ECR nitrogen plasma. In addition, the BP film was exposed to a nitrogen atmosphere in which a tungsten filament, heated to about 2300°C, was used to thermally dissociate the nitrogen molecules. In the latter case, diamond nucleation on the converted film was subsequently attempted.

## B. Experimental Procedure

Epitaxial BP films on both Si (100) and Si (111) were grown by Professor Kumashiro's research group at Yokohama National University in Japan. X-ray diffraction confirmed that they are single crystal BP films with a lattice constant of 4.538Å. The nitrogen plasma was generated by a unique ECR plasma source which was designed and constructed inside a 2.25" diameter tube on a commercial Perkin-Elmer 430 MBE system's source flange cryoshroud. The details of this system can be found elsewhere [6]. Ultra high purity nitrogen, further purified by a chemical purifier, was used as the source gas. The conditions of the nitrogen plasma used in this study are as follows: flow rate of nitrogen is about 5sccm and the ECR plasma power is about 50W, the distance between film and plasma source is about 15cm. During the nitrogen plasma exposure, the samples were heated to 400°C.

For the experiments involving thermal dissociation of nitrogen molecules by a heated tungsten filament, the BP film was radiatively heated to a temperature of 750°C by placing the film about 1 cm away from the filament, which was heated to about 2300°C. The exposure to nitrogen lasted 30 minutes. Then, diamond nucleation was attempted under the conditions of 0.3%$CH_4$ in $H_2$, a pressure of 30 torr and a total flow rate of 600 sccm. The substrate temperature was kept at 700°C. The diamond nucleation lasted 160 minutes. Raman spectroscopy was performed on the sample to verify if diamond nucleation had occurred.

C. Results

The boron phosphoride films, prior to and after exposing to the nitrogen plasma, were mainly characterized by X-ray photoelectron spectroscopy (XPS) analysis, which is connected to the MBE system. XPS spectra were obtained with a Riber Mg/Al XPS X-ray source and a Riber MAC II cylindrical electron analyzer. Spectra data were acquired by an IBM PC-AT running software developed at NCSU.

Figure 1 shows an XPS spectra for the BP film on Si (100) before and after a 1.5 hour exposure to the nitrogen plasma. The results indicated that a strong nitrogen peak centered at 397.9 eV ($N_{1s}$) occurred in the film after exposure to the nitrogen plasma. To investigate the effect on the boron and phosphorus peak positions, we re-acquired data within the binding energy range between 110 to 210 eV, as shown in Fig. 2. As indicated in the spectra, with an increase in the exposure time, the $B_{1s}$-peak position has shifted from a BP bonded peak (192.5 eV) to a BN bonded peak (195 eV). While the intensity of the $P_{2p}$-peak was reduced a shoulder peak started to show up, which could be either another $P_{2p}$ peak or a $P_3N_5$ peak. All of this indicated that after exposure to the nitrogen plasma, the surface of the BP film has been successfully converted to BN. A similar study has also been conducted for a BP film on Si (111). The results were very similar, in addition the nitradation rate of the BP surface on Si (111) is much faster than on Si(100).

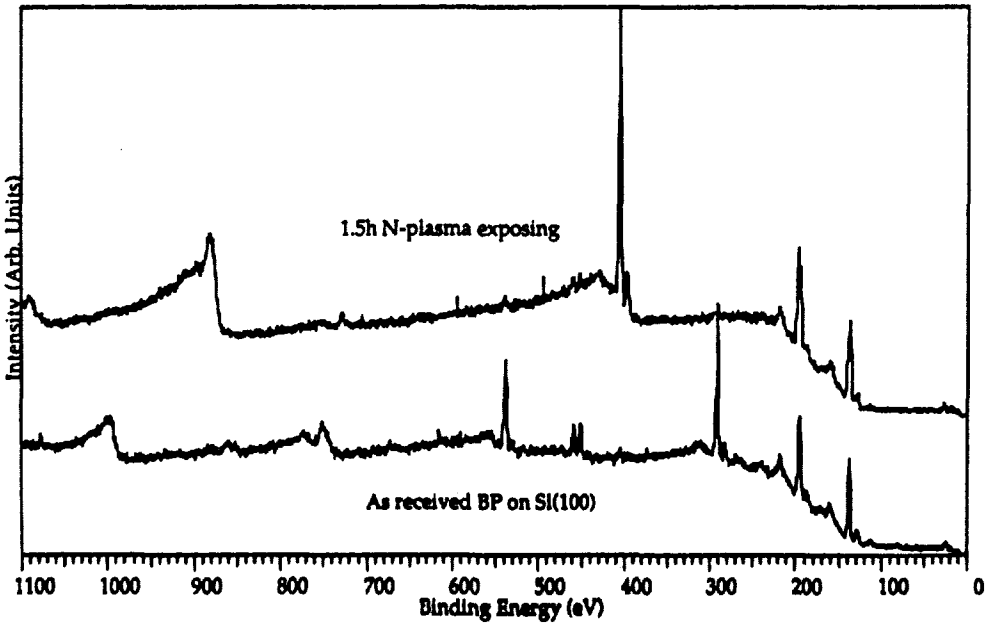


Figure 1. XPS spectra for the BP film on Si (100) before and after 1.5 hour nitrogen plasma exposing.

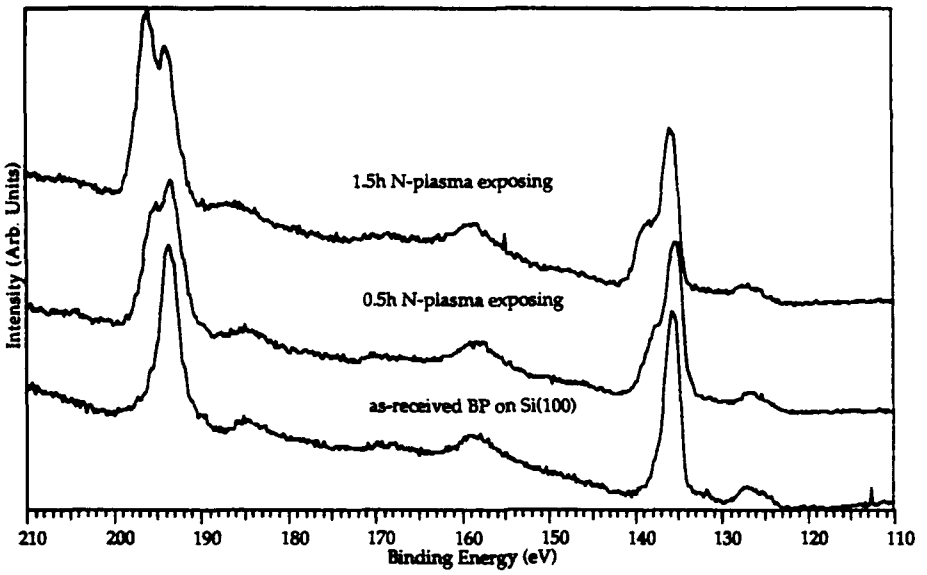


Figure 2. XPS spectra for BP on Si (100) before and after nitrogen plasma exposing.

In order to determine the nature of the BN layer on the surface of the BP film, we have taken FTIR measurements. However, due to the detection limit of the instrument, the structure of this BN layer cannot be determined since only the very top layer of the BP film has been converted to BN. Further study is under way to determine the structure of this BN by using high resolution TEM.

We have also conducted initial electrical characterization for these converted films. IV measurements of BP on Si (100) have been taken before and after exposure to the nitrogen plasma. The results indicate that the films become more resistive, an increase of approximately a factor of 40, after exposure to the nitrogen plasma for about 1.5 hours.

For a sample which has undergone diamond nucleation after the attempted thermal conversion of BP to cBN, Raman spectroscopy confirmed that an amorphous carbon layer was deposited on the substrate surface which showed a broad peak at 1520 $cm^{-1}$, as indicated in Fig. 3. Further experiments will be performed by using different substrate temperatures and time durations for the conversion of BP and cBN. More careful characterization of the films including SEM and XRD will also be conducted.

D. Future Studies

Further investigation needs to be conducted to determine the nature of the converted BN layer in order to make this process practical for the epitaxial growth of cubic boron nitride films. Also, the effect of the plasma conditions on the converting process, such as plasma power, nitrogen flow rate and substrate temperature, need to be studied.

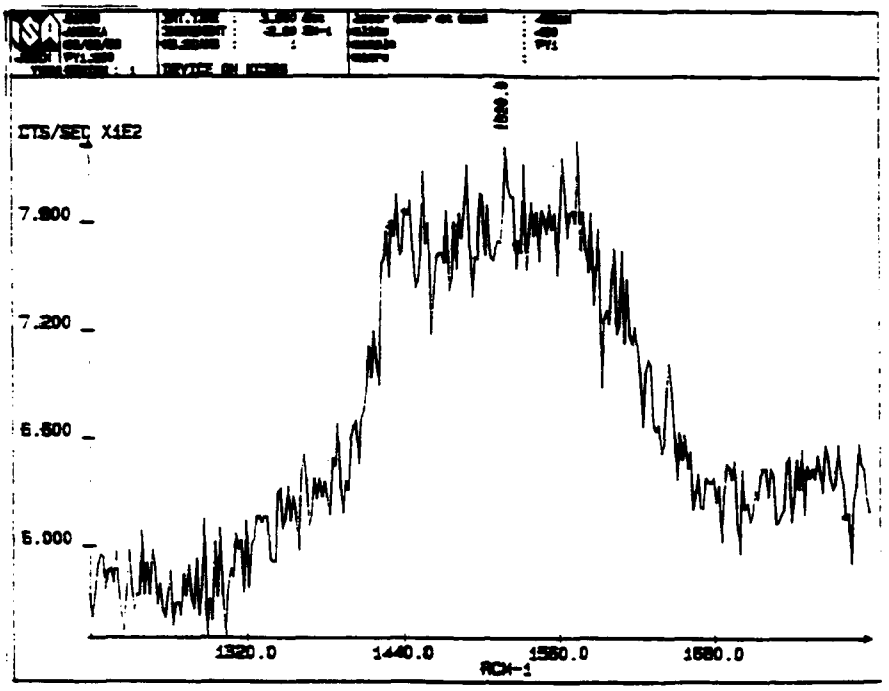


Figure 3. Raman spectrum from the sample which underwent thermal conversion of BP to cBN and diamond nucleation.

References

1. Y. Hirai and K. Shohno, J. Cryst. Growth **41**, 124-132 (1977).
2. K. Shohno, H. Ohtake and J. Bloem, J. Cryst. Growth **45**, 187-191 (1978).
3. K. Nonaka, C. J. Kim and K. Shohno **50**, 549-551 (1980).
4. Y. Kumashiro, Y. Okada and S. Gonda, J. Cryst. Growth **70**, 507-514 (1984).
5. R. J. Baughman and D. S. Ginley, J. Solid State Chem. **50**, 189-195 (1983).
6. Z. Sitar, M. J. Paisley, D. K. Smith and R. F. Davis, Rev. Sci. Instrum. **61**, 2407 (1990).

# V. Contact Formation in GaN and AlN

## A. Introduction

The III-V nitrides have long been known to possess properties that have potentially great technological value. These materials can be considered as largely covalent ceramics, whose unique combinations of properties are only beginning to be put to use. For electronic and optoelectronic device applications, the most important characteristics of the III-V nitrides are that they are all semiconductors having wide, direct bandgaps and form complete solid solutions with one another. With the bandgap of GaN being 3.4 eV and that of AlN 6.28 eV, the possibility exists for optical and optoelectronic devices active from the blue region of the electromagnetic spectrum to well into the ultraviolet. To date, semiconductor devices have been developed that operate in the infrared to green regions of the spectrum, but as yet attempts to push this capability to shorter wavelengths have been unsuccessful. The present study is part of an effort to characterize the semiconductor and optical properties of the III-V nitrides, and to demonstrate the valuable technological capabilities of these materials.

The formation of good ohmic and rectifying (Schottky) contacts is a fundamentally important technological step in the fabrication of working semiconductor devices. Extensive coverage of contact formation to GaAs can be found in the literature[1–5]; studies of other III-V semiconductors are much fewer, although some work on GaN has been reported [6]. Multiple avenues of this subject will be explored, including the effects of subsequent annealing on the contact behavior, cross-sectional examination of interfaces via transmission electron microscopy (TEM), and probing the metal-semiconductor surface using spectroscopic techniques such as x-ray photoelectron spectroscopy (XPS).

In order to take full advantage of the properties of a semiconductor and connect it to other components, it must be possible to make both ohmic and rectifying (Schottky) contacts to the material with appropriate conductors. For the compound semiconductors, particularly those with mostly covalent bonding, the art of perfecting the properties of both types of interfaces has been found to be a challenging one. It has become plain that there are many factors, particularly interface reaction chemistry and morphology, that significantly affect the physical and electronic behavior of contacts. Many of these factors are only beginning to be understood and documented, even for the now-conventional compound semiconductors such as GaAs.

The most important property of an ohmic contact for device operation is the inherent contact resistance of the interface; for a Schottky contact the key parameter is the height of the rectifying barrier, or Schottky barrier height. Over the years a variety of methods have been developed for measuring these parameters [7]. For the purposes of this study of fundamental interface characteristics, simple contact configurations are being used in order to minimize the need for multiple patterning steps and the complex chemical exposures such processing would

entail. For contact resistance measurements of ohmic contacts, transfer length measurements (TLM) are commonly used in device technology and are employed in this study, along with current-voltage (I-V) measurements. Capacitance-voltage (C-V) measurements as well as I-V measurements will be used for Schottky barrier height determination. The thermal stability of the contacts will also be investigated by characterization following annealing treatments.

B. Experimental Procedure

*Contact Deposition.* For this first set of contact experiments, Pt was chosen as the material for Schottky contacts on n-type GaN and ohmic on p-type films; TiN was chosen for the opposite relationship, ohmic on n-type GaN and Schottky on p-type. Some properties of these materials are listed below in Table I. Both Pt and TiN were chosen for their relative chemical inertness and refractory character; in terms of the Schottky-Mott-Bardeen model of metal-semiconductor interfaces [8], Pt was intended to serve as the high work function metal and TiN for the low work function material.

Table 1. AlN/GaN Contact Candidates

| | AlN | GaN | TiN | Pt |
|---|---|---|---|---|
| **symmetry** | hexagonal | hexagonal | NaCl | fcc |
| **lattice param. (Å)** | a: 3.112<br>c: 4.982 | a: 3.189<br>c: 5.185 | a: 2.998*<br>$a_0$: 4.240 | a: 2.775*<br>$a_0$: 3.924 |
| **work function (eV)** | 5.35 | 4.1 | 3.74 | 5.65 |
| **surface energy ($mJ/m^2$)** | 990±110 | | | 2691 |

* Nearest neighbor distance (a-plane for hexagonal; (111) for fcc)

Gallium nitride films approximately 3000Å thick were deposited on 6H-SiC substrates (Cree Research, Research Triangle Park, NC) by means of gas-source molecular beam epitaxy (MBE) assisted by an electron-cyclotron resonance (ECR) plasma generator; the equipment, substrate preparation, and growth parameters are described elsewhere in this report. After the GaN deposition, each sample was briefly removed from the vacuum system to affix a shadow mask prior to the deposition of the contact layer. Two different shadow masks were used, to create contact patterns for transfer length measurements (TLM) of ohmic contact candidates and Schottky diode measurements of Schottky contact candidates. For the deposition of Pt and TiN, a UHV electron-beam evaporation system was used. The metals were evaporated onto room-temperature substrates using Thermionics HM2 electron guns with swept beams at deposition rates of 4 to 20 Å/min. For TiN deposition, a Kaufman type ion gun was used to activate the nitrogen gas for nitride formation. The deposition rate of Ti, the energy and flux of ions, and the substrate temperature were all measured and controlled. Deposition rates were monitored using a quartz crystal oscillator.

*Contact Characterization.* Current-voltage (I-V) measurements were performed on the samples using a Hewlett-Packard 4145C Semiconductor Parameter Analyzer. Tungsten probes attached to x-y-z manipulators under a low-power microscope were used to collect data from the samples. During data collection, the voltage between the probes was swept from –10 to +10 V. The resulting I-V curves were plotted by a Hewlett-Packard pen plotter, and some were later digitized for Macintosh graphics formatting using *Ofoto v. 2.0* scanning software.

Scottky diode I-V measurements were taken by applying the probes to combinations of large- and small-area circular dot contacts on the top surface of each sample, and to small dots in combination with a back-plane contact formed by the sample wafer affixed by vacuum suction to a copper block. The contact pattern for ohmic contact resistance measurements using the transmission line model (TLM) method [9,10] consisted of arrays of long rectangular bars, of fixed size (30×150 μm) and varied separation distance.

C. Results

Current-voltage and log I-V measurements of Pt Schottky dot contacts on n-type GaN did reveal the contacts to be rectifying, whether measured through the thickness using a back-plane contact, or across two surface dots of different size. Typical I-V and log I-V plots for back-plane contact measurements are shown in Fig. 1. The behavior of the top surface contacts was similar, but revealed less ideal diode behavior, higher turn-on voltages, and somewhat more reverse bias leakage. From the log I-V plots, ideality factors and barrier heights were calculated, as described by Sze [11]:

$$\text{Ideality factor } n=(q/kT)(\partial V/\partial \ln J)$$

$$\text{Barrier height } \phi_b=(kT/q)\ln(A^*T^2/J_s)$$

where $A^*$ is the effective Richardson constant for the semiconductor; for this parameter, a value for low-mobility n-GaAs was used ($3\times10^4$ A/m$^2$K$^2$). For the Pt on n-GaN samples, ideality factors ranged from n=1.7 to 2.0 and barrier heights from $\phi_b$=1.03 to 1.09 V.

(a)

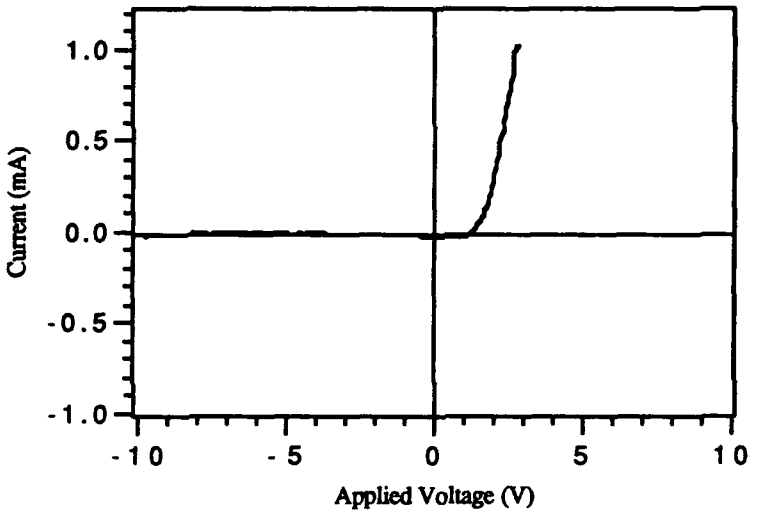


(b)

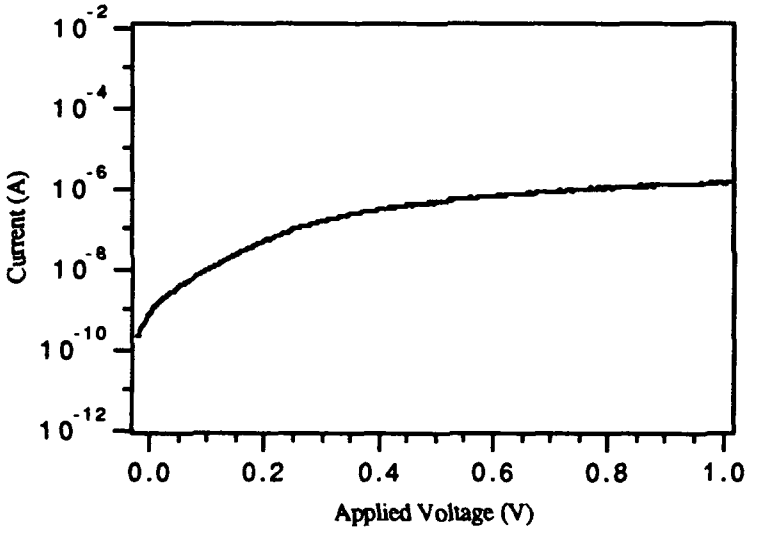


Figure 1. Typical (a) current-voltage and (b) log current-voltage measurements of Pt/n-GaN contacts taken using a small dot-back plane contact combination.

Platinum contacts deposited on p-type GaN did not exhibit ohmic behavior in the as-deposited state. Current-voltage measurements taken across pairs of top contacts and through the back-plane contact revealed less-than-ideal, "leaky" rectifying behavior. Since an ohmic I-V relationship did not exist across the contact interface, it was not possible to take contact resistance measurements using the TLM pattern.

D. Discussion

Platinum contacts deposited on both n-type and p-type GaN were found to be rectifying in the as-deposited state. The nonideality of the I-V and log I-V relationships indicates that a variety of current transport mechanisms were at work. The fact that the Pt/p-GaN contact was rectifying, despite a work function relationship that was favorable to ohmic contact formation, indicates the presence of a potential barrier at the interface.

Experimentally it has been found that the barrier height for a given metal-semiconductor interface is not very dependent on the choice of metal. The presence of additional electron states at the interface can significantly change the junction's electron energy structure; the origins of and mechanisms behind these states are not yet completely understood. Over twenty years ago Kurtin *et al.* described the correlation between the ionicity of a semiconductor's atomic bonding —*i.e.* the relative difference in electronegativity between the elements in a compound—and its surface and interface behavior [12]. The lattice electronegativity differences for GaN and AlN are 1.23 and 1.43, respectively, which correspond to bond ionicities of approximately 32% and 40%. These properties make GaN and AlN significantly more ionic in nature than the more conventional semiconductors; consequently, it is hoped that GaN and AlN will be more sensitive to metal work function differences than the more covalent semiconductors have been.

It has been observed that improving the chemical and morphological abruptness of an interface and making a close match of thermal and mechanical properties is helpful for improving the performance of rectifying contacts. By the same token, extending a gradation of composition and properties at the interface generally improves ohmic contacts. A thin layer of Ti, capped with a thicker layer of Au and then subsequently annealed, is an ohmic contact system that has met with success on a variety of n-type semiconductors over the years, and presents itself as a likely candidate for study. In this study, the next experimental step is to investigate the effects of annealing treatments on the properties of the contacts, in addition to depositing different materials and combinations of materials. Depositions of TiN on both n- and p-type GaN will be conducted shortly.

E. Conclusions

In the as-deposited state, Pt contacts deposited on n-type and p-type GaN have been found to be rectifying in both cases. The I-V and log I-V measurements of the contacts yielded high

ideality factor values, indicative of the presence of a variety of current transport mechanisms, and barrier heights of just over 1 eV. These experiments are the first steps in a systematic study of ohmic and Schottky contact formation to GaN and AlN, in which a variety of contact materials will be investigated and a variety of processing and characterization strategies will be brought to bear.

F. Future Plans and Goals

Annealing treatments will be conducted to study the effects of temperature, diffusion, and chemical reactions on the contact interfaces. The thermal stability of a contact is an important characteristic that may place restrictions on device processing parameters and materials selection; in some cases annealing treatments are required to achieve better device characteristics, and in other cases heating steps can cause serious degradation of properties. Electrical characterization of samples by means of I-V and log I-V measurements, capacitance-voltage (C-V) measurements, and Hall effect measurements will be performed. Band structures will be studied by means of electrical measurements, luminescence techniques, and ultraviolet photoelectron spectroscopy (UPS). Structural and chemical characterization will be accomplished by means of high resolution scanning electron microscopy (SEM), X-TEM, XPS, and Auger electron spectroscopy (AES).

Aside from further study of the Pt/GaN and TiN/GaN systems, there are a number of other metalization choices that will be investigated. Titanium-gold and AuGe/Au layered structures are examples of ohmic contact strategies that have been applied with some success to GaAs and other compound semiconductors, and will be examined as likely candidates. Other metals besides Pt, such as Au, Ni, W, Ru, and Re are possible candidates for Schottky contacts. Khan *et al.* recently reported the fabrication of a GaN metal semiconductor field effect transistor (MESFET), using annealed Ti/Au layers as the ohmic source and drain contacts and Ag for the gate Schottky contact [13]. The development of the III-V nitrides as semiconductor device materials is a field that is beginning to move rapidly, and the current literature will be studied closely to keep abreast of any new findings.

G. References


1. M. Murakami, Materials Science Reports (5) 273 (1990).
2. A. Piotrowska and E. Kaminska, Thin Solid Films **193/194** 511 (1990).
3. T. C. Shen, G. B. Gao, H. Morkoç, J. Vac. Sci. Technol. B **10**(5) 2113 (1992).
4. J. Ding, Z. Liliental-Weber, E. R. Weber, and J. Washburn, Appl. Phys. Lett. **52**(25) 2160 (1988).
5. G. Myburg and F. D. Auret, Appl. Phys. Lett. **60**(5) 604 (1992).
6. J. Foresi, *Ohmic Contacts and Schottky Barriers on GaN*, M.S. Thesis, Boston University (1992).
7. H. K. Henisch, *Semiconductor Contacts*. (Clarendon Press, Oxford, 1984).

8. E. H. Rhoderick, *Metal-Semiconductor Contacts* (Oxford University Press, New York, 1988).
9. H. H. Berger, Solid State Electronics **15**(2-A) 145 (1972).
10. G. K. Reeves and H. B. Harrison, IEEE Electron Device Lett. **EDL-3** 111 (1982).
11. Sze, *Physics of Semiconductor Devices*, 2nd ed. (John Wiley and Sons, New York, 1981).
12. S. Kurtin, T. C. McGill and C. A. Mead, Phys. Rev. Lett. **22**(26) 1433 (1969).
13. M. Asif Khan, J. N. Kuznia, A. R. Bhattarai, and D. T. Olson, Appl. Phys. Lett. **62**(15) 1786 (1993).

# VI. Reactive Ion Etching of GaN and AlN

## A. Introduction

Semiconductor devices are the principle components of electronic and telecommunications systems [1]. In order to densely pack these microscopic components, unidirectional, or anisotropic, etching techniques are required to produce a fine network of lines. Wet etching processes found in many semiconductor manufacturing steps produce a multi-directional, or isotropically, etched material. This is undesirable for microcircuitry since the goal is to produce the smallest devices possible. Therefore, plasma-assisted processes, such as reactive ion etching (RIE), combine the physical characteristics of sputtering with the chemical activity of reactive species to produce a highly directional feature. RIE has the added advantage of providing a more uniform etch and a higher degree of material etch selectivity.

RIE has been employed to etch a wide variety of semiconductor materials including silicon-based materials [2–11], metals, like aluminum [3, 12–18] and III-V compounds, such as GaAs and InP [19–21]. However, plasma-assisted etching of newer III-V compounds, such as GaN and AlN, has been attempted by few investigators [20, 21, 37]. There has been wide spread interest in using these nitrides for semiconductor device applications requiring visible light emission, high temperature operation and high electron velocities [20]. Since these materials possess wide bandgaps and optical emissions spectra in the blue to near ultraviolet range, they are prime candidates for ultraviolet detection devices.

The objectives of this report are to discuss recent progress made in the field of reactive ion etching of gallium and aluminum nitride and to describe the reactive ion etching system. A long term goal is to develop and characterize suitable processes for the anisotropic etching of these nitrides. In the following sections, a brief review of pertinent literature on plasma-assisted etching of gallium and aluminum compounds is provided along with a brief description of the reactive ion etching system.

## B. Literature Review

*Reactive Ion Etching of GaN.* Since GaN is a direct transition material with a bandgap ranging from 3.4–6.2 eV at room temperature, it is an ideal candidate for the fabrication of shortwave length light emitters [20, 22]. High quality GaN films have been successfully grown by MOVPE [22], ECR-MBE [23, 24], MOCVD [25] and a layer-by-layer process [26] on a number of substrate. In order to fabricate complete device structures, reliable etching processes need to be developed. Since GaN is nearly inert to most wet etching solutions, with the exception of highly concentrated hot NaOH and $H_2SO_4$ [27], RIE may prove to be an effective method for the production of fine line patterning in semiconductor materials.

There have been a few reports of etching GaN by plasma-assisted processes [20, 21, 37].

Foresi [21] investigated fabrication techniques for ohmic contact and schottky barriers on GaN. One of the highlights of his work was the successful etching of GaN on sapphire substrate in Freon 12 ($CCl_2F_2$) and in hydrogen atmospheres operating at about 10 mTorr and 40 and 60 W of RF power. Results from SEM photographs showed that in the $CCl_2F_2$ plasma, GaN had been completely removed from areas that were not covered by photoresist, and that the sapphire substrate was nearly unetched. Foresi was able to obtain an etch rate of approximately 140 Å/min in the $CCl_2F_2$ plasma at 60 W, while the hydrogen plasma produced insignificant etching results. Etch selectivity between the GaN and photoresist was found to be 3:1. In another investigation, conducted by Tanaka et al. [20] reactive fast atom beam etching was employed to etch GaN on sapphire in a $Cl_2$ plasma at substrate temperatures ranging between 80–150°C. Etch rates of 1000–1200 Å/min produced relatively smooth surfaces and a well defined pattern of elongated rectangular bars on the sapphire substrate. More recently, S. J. Pearton *et al.* [37] have produced smooth, anisotropically etched GaN and AlN in low pressure ECR discharges of $BCl_3$/Ar, $CCl_2F_2$/Ar and $CH_4/H_2$/Ar. The etch rates of these nitrides was highly dependent on the DC bias voltage and ranges of 25–175 Å/min and 0–100 Å/min were reported for GaN and AlN, respectively. It is noted that hydrogen was added to the chlorine plasmas to facilitate removal of hydrogen from the surfaces of the nitride samples, thus producing smoother features.

*Reactive Ion Etching of AlN.* Aluminum nitride is a candidate material for optoelectronic devices because it possesses a high electrical resistivity, high thermal conductivity, low dielectric constant and has a direct transition bandgap of 6.3 eV [28]. AlN films have been grown by several techniques including CVD, MBE and ALE, and on a variety of substrate materials including sapphire, silicon, spinel, silicon carbide and quartz [29]. Etching fine features in the AlN films is an important step in the fabrication of such devices. Though, only one report of etching of AlN is available in the open literature at this time [37], much work has been conducted on etching of metallic aluminum thin films [3, 12–18]. As a result, analogies to well established data for etching of aluminum are made. Although aluminum and AlN are very different materials, the chemistry and reactions in the plasma may be similar. So, it is proposed that reactive ion etching may also be an effective means for the application of fine line patterning of AlN.

A review of the literature shows that there are two primary methods employed for etching aluminum. Bruce and Malafsky [12] employed a parallel plate configuration (RIE) to investigate the effects of $Cl_2$ on aluminum. They found that two processes are involved, namely, the removal of the oxide layer and etching the metal below it. For those experiments, it was hypothesized that $BCl_3$ gas was necessary for the removal of the oxide layer because it was responsible for the initiation of a reduction reaction with the oxide. In the RIE etching configuration, aluminum etched with a chlorinated gas is a purely chemical reaction with little

contribution from ion bombardment. This conclusion was made as a result of the insensitivity of RF power to the etch rate [12]. Therefore, anisotropic etching was thought to have been the result of a sidewall passivation mechanism whereby a protective layer is formed on the vertical walls of the trench by reaction of $H_2O$ or carbon containing species with the aluminum. Since ion bombardment is normal to the surface, the walls remained unetched. This mechanism was produced by the addition of $CHCl_3$ to the mixture of gases. Feature widths of 2.25 μm were produced by a gas mixture of $Cl_2$, $BCl_3$, $CHCl_3$ and He at about 1.2 mTorr. Helium gas was added to the mixture to reduce the amount of erosion of the photoresist.

The combination of an isotropic flux of reactive species with a highly directional beam of energetic ions, so called ion beam assisted etching (IBAE), has been employed for the anisotropic etching of aluminum by many investigators [13–15, 18]. For IBAE, the aluminum oxide layer can be physically removed by sputtering with $Ar^+$ or $Xe^+$ ions, whereas with RIE the oxide is removed chemically [13]. However, etching takes place again by chemical reaction of $Cl_2$ with the aluminum as determined by the lack of dependence of the etch rate on the ion energy and current [14, 15]. From a mechanistic point of view, $Cl_2$ adsorbs onto and diffuses into the aluminum resulting in the formation of aluminum chlorides. $Al_2Cl_6$ is the dominant etch product at lower temperatures (33°C), while $AlCl_3$ was observed at higher temperatures (210°C) [15]. Saturation of the etched surface with chlorine atoms occurs prior to desorption of $AlCl_3$.

The etch rate is dependent upon several parameters including the presence of residual gases in the chamber, substrate temperature, $Cl_2$ flux, ion beam and the presence of carbon containing species. Impurity gases in the chamber (i.e. $H_2O$, $O_2$, $N_2$, etc.) can react with the aluminum films and impede the etching process by leaving a residue on the etched surface. This reduces the amount of $Cl_2$ available for reaction and consequently lowers the etch rate [13]. The substrate temperature is another parameter that affects the etch rate of aluminum. Efremow *et al.* [13] observed a two-fold increase in the etch rate by heating the substrate from 0° to 100°C. It was hypothesized that the increase in temperature led to a higher evaporation rate of the product $AlCl_3$. In addition, they found that an increase in the $Cl_2$ flux produced a significant amount of undercutting due to the nondirectional flow of the $Cl_2$ gas. A higher degree of anisotropy was achieved by the combination of ion beam and $Cl_2$ flux. Efremow *et al.* suggested that sidewall passivation (by reaction of $H_2O$ with the aluminum) was partly responsible for the production of the very fine features in their samples. Submicrostructures of 80 nm wide lines were etched into a 100 nm thick aluminum film with 0.3 mTorr $Cl_2$ gas and 0.1 mA, 1 keV $Ar^+$ beam. Lastly, Parks *et al.* [14] found that chemisorption of the halocarbon gas molecules, such as $CCl_4$ and $CBr_4$, onto the aluminum surface formed halogentated aluminum species along with an aluminum carbide. Therefore, a significant reduction in the etch rate was observed due to the difficulty encountered in removing the carbide from the surface.

C. Proposed Research

*Experimental Apparatus*. Since the date of the last report [38], the design of the RIE system has been changed in the interest of constructing a more cost-effective, reliable and safe system. Since toxic gases, such as $BCl_3$ and $Cl_2$, may be used to etch GaN and AlN, the system is designed for safe shutdown in the event of a power or water failure and/or inadvertent shutdown of the exhaust systems in the building. The main components of the system include gas handling/storage, etcher, gas scrubber and mass spectrometer. A schematic of the RIE system is shown in Fig. 1.

**Figure 1. Schematic Diagram of the Reactive Ion Etching System**

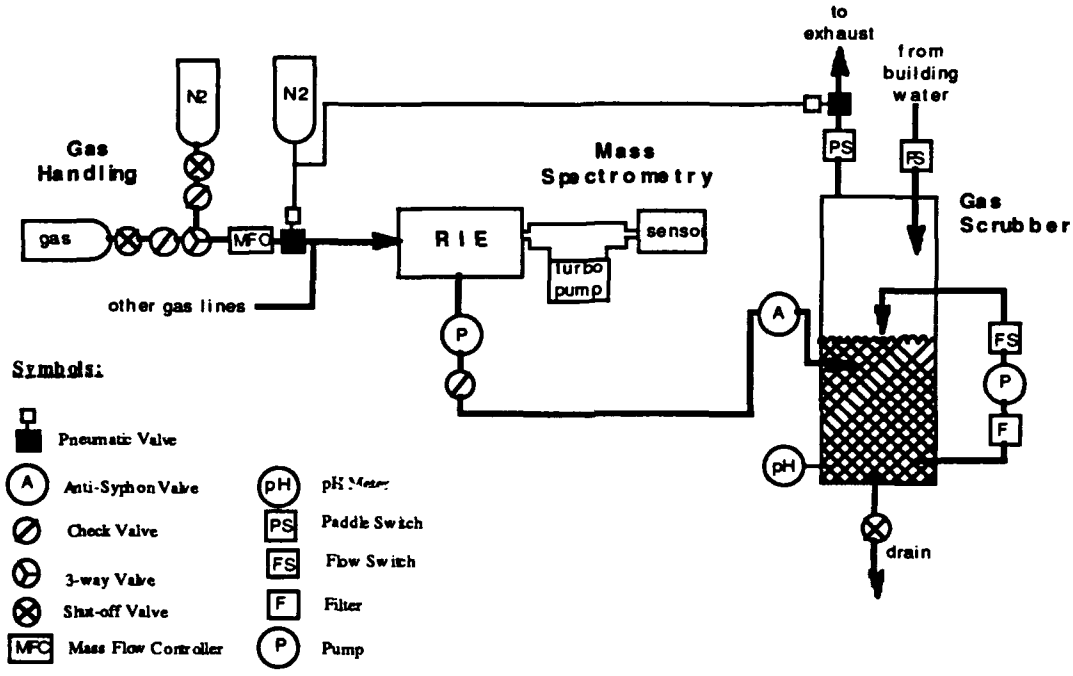


The gas handling/storage sub-system consists of the gas storage cabinet(s), gas bottles, bottle regulators and necessary valves and tubing. Dry nitrogen will be used to purge the gas lines before and after every run to remove moisture and chlorine from the lines, thus reducing the probability of corrosion of the gas lines. Mass flow controllers will be employed for accurate control of the process gases. In addition, pneumatic valves will be installed as a safety precaution. In the event of a power failure, interruption of the water supply or shutdown of the exhaust system, the solenoid actuated pneumatic valves will isolate the gas lines from the etch chamber.

The design of the etcher is based on that of the standard parallel-plate diode configuration in which the bottom electrode is powered by a RF power supply (see for example Ref. 10). The

etcher, a Technics 85 series RIE, consists of an anodized aluminum chamber with an anodized aluminum water-cooled, driven lower electrode. A 350 Watt, 13.56 MHz RF generator with auto impedance matching network produces the power required to maintain a glow discharge in the chamber. Safety interlocks are supplied by Technics to disable the power when the system is vented or a panel is removed. The chamber pressure is measured by a corrosion-resistant capacitance manometer (absolute pressure) which is mounted to the underside of the chamber. The two channels of process gas (made from stainless steel tubing) are isolated from the injection manifold by means of air-operated electrically actuated isolation valves. In addition, an 11 CFM two-stage corrosive-series direct drive rotary vane pump is supplied with the etcher.

Residual process gases and reaction by-products from the etcher will pass through a wet scrubber which is equipped with water inlet and water recirculation lines. These lines are monitored by flow switches, and the exhaust line is monitored by a paddle switch. Interruption of the water flow or inadequate ventilation will trip the pneumatic valves and close the gas lines. An anti-siphon valve is incorporated into the design to ensure there is no backflow of water from the scrubber into the pump exhaust. In addition, the pH level of the scrubber water will be tested and monitored prior to waste disposal.

Lastly, a mass spectrometer may be employed in the future for the detection and characterization of chemical species produced by the etching processes. It could also be used as a kind of end-point detection device. It is further hoped that this analytical instrumentation could provide necessary information for the determination of the success of the etching processes and could provide a basis for an understanding of the etching mechanisms.

*Choice of Process Gases.* There are a number of process gases that can be used to produce anisotropically etched features. For GaN and AlN, fluorine plasmas are impractical because involitile fluorides are formed at the surfaces, therefore limiting desorption of reaction species from the surface [35]. Chlorine plasmas, on the other hand, have been used extensively for etching these compounds, see Section B above.

In etching GaN, the gases used by Tanaka [20], Foresi [21] and S. J. Pearton *et al.*[37] namely $CCl_2F_2$, $Cl_2$ and $BCl_3$ will be employed first since those investigators reported successful results. Experimentation with other combinations of gases is likely in order to obtain anisotropic features and reasonably high etch rates. As for AlN, chlorine containing gases with additions of $O_2$, carbon containing gases and or noble gases (i.e. Ar, He, etc.) are likely candidate gases. Though, somewhat of a trial and error methodology will be followed until success is achieved. It is noted that for RIE, sidewall passivation may be an important mechanism for anisotropic etching of AlN and may produce relatively large features. On the other hand, ion beam assisted etching, or similar techniques, are likely to produces smaller features in these nitrides.

D. Future Research

Future plans include installation of the RIE system and development and characterization of suitable etching processes for aluminum and gallium nitride materials.

E. References


1. *Plasma Processing of Materials: Scientific Opportunities and Technological Challenges, Panel on Plasma Processing of Materials*, National Research Council (National Academy Press, Washington, D.C., 1991).
2. J. W. Palmour, R. F. Davis, T. M. Wallett and K. B. Bhasin, J. Vac. Sci. Technol., **A4**, 590 (1986).
3. D. L. Smith, P. G. Saviano, J. Vac. Sci. Technol. **21**, 768 (1982).
4. D. L. Smith and R. H. Bruce, J. Electrochem. Soc. **129**, 2045, (1978).
5. C. J. Mogab, A. C. Adams and D. L. Flamm, J. Appl. Phys. **49**, 3796 (1978).
6. S. Matsuo, J. Vac. Sci. Technol. **17**, 587 (1980).
7. L. M. Ephrath, Solid State Technol., July 1982, p. 87.
8. Y.H. Lee and M. M. Chen, J. Appl. Phys. **54**, 5966 (1983).
9. L. M. Ephrath, J. Electrochem. Soc., August 1979, p. 1419.
10. A. J. van Roosmalen, Vacuum **34**, 429 (1984).
11. M. Zhang, J. Z. Li, I. Adesida and E. D. Wolf, J. Vac. Sci. Technol. **B1**, 1037 (1983).
12. R. H. Bruce and G. P. Malafsky, J. Electrochem. Soc. **136**, 1369 (1983).
13. N. N. Efremow, M. W. Geis, R. W. Mountain, G. A. Lincoln, J. N. Randall and N. P. Economou, J. Vac. Sci. Technol. **B4**, 337 (1986).
14. S. Park, L. C. Rathburn and T. N. Rhodin, J. Vac. Sci. Technol. **A3**, 791 (1985).
15. H. F. Winters, J. Vac. Sci. Technol. **B3**, 9 (1985).
16. D. A. Danner and D. W.Hess, J. Appl. Phys. **59**, 940 (1986).
17. R. J. A. A. Janssen, A. W. Kolfschoten and G. N. A. van Veen, Appl. Phys. Lett., **52**, 98 (1988).
18. Y. Ochiai, K. Shihoyama, T. Shiokawa, K. Toyoda, A. Masuyama, K. Gamu, S. Namba, J. Appl. Phys. **25**, L527 (1986).
19. G. Smolinski, R. P. Chang and T. M. Mayer, J. Vac. Sci. Technol. **18**, 12 (1981).
20. H. Tanaka, Optoelectronics - Devices and Technologies **6**, 150 (1991).
21. J. S. Foresi, M. S. Thesis, Boston University, Boston, MA, 1992.
22. I. Akasaki and H. Amano, "Conductivity control of AlGaN, fabrication of AlGaN/GaN multi-heterostructure and their application to UV/Blue light emitting devices," July 1992 MRS conference.
23. C. Eddy, Ph.D. Thesis, Boston University, Boston, MA, 1990.
24. T. Lei and T. D. Moustakas, J. Appl. Phys. **71**, 4933 (1992).
25. Z. J. Yu, B.S. Sywe, A. U. Ahmed, J. H. Edger, J. Electr. Mater. **21**, 782 (1992).
26. J. Sumakeris, Z. Sitar, K. S. Ailey-Trent, K. L. Moore and R. F. Davis, "Layer-by-Layer Epitaxial Growth of GaN at Low Temperatures," (to be published in Thin Solid Films).
27. *CRC Handbook of Metal Etchants*, eds. P. Walker and W. H. Tarn (CRC Press, Boca Raton, LA, 1991).
28. E. S. Dettmer, B. M. Romenesko, H. K. Charles Jr., B. G. Carkhuff and D. J. Merrill, IEEE Transactions - Components, Hybrids, Manuf. Technol., **12**, 543 (1989).
29. L. B. Rowland, Ph.D. Thesis, North Carolina State University, Raleigh, NC, 1992.
30. D. Suryanarayana, J. Am. Cer. Soc. **73**, 1108 (1990).
31. A. D. Katnani and K. I. Papathomas, J. Vac. Sci. Technol. **A5**, 1335 (1987).
32. A. Abid, R. Bensalem and B. J. Sealy, J. Mater. Sci. **21**, 1301 (1986).
33. T. Sato, K. Haryu, T. Endo and M. Shimado, J. Mater. Sci. **22**, 2277 (1987).
34. D. Suryanarayana, L. J. Matienzo and D. F. Spencer, IEEE Transactions - Components, Hybrids, Manuf. Technol. **12**, 566 (1989).

35. V. M. Donnelly and D. L. Flamm, Solid State Technol., April 1981, p. 161.
36. G. S. Oehrlein, in *Handbook of Plasma Processing Technology*, eds. S.M. Rossnagel, J. J Cuomo and W. D. Westwood, (Noyes Publications, Park Ridge, New Jersey, 1990).
37. S. J. Pearton, C. R. Abernathy, F. Ren, J. R. Lothian, P. W. Wisk, A. Katz and C. Constantine, Semiconductor Sci. Technol. **8**, 310 (1993).
38. R. F. Davis, K. S. Ailey-Trent, D. Kester, R. Patterson, W. Perry, L. Smith, C. Wang, W. Weeks, K. Webber, "Nitride Semiconductors for Ultraviolet Detection," Annual Report, December 1992, p. 44.

# VII. Development of Photo- and Cathodoluminescence System for Optical Studies of III-V Nitride Films

## A. Introduction

Luminescence is the emission of photons due to excited electrons in the conduction band decaying to their original energy levels in the valance band. The wavelength of the emitted light is directly related to the energy of the transition, by E=hν. Thus, the energy levels of a semiconductor, including radiative transitions between the conduction band, valance band, and exciton, donor, and acceptor levels, can be measured [1,2].

In luminescence spectroscopy various methods exist to excite the electrons, including photoluminescence (photon excitation), and cathodoluminescence (electron-beam excitation). In each technique signal intensity is measured at specific wavelength intervals using a monochrometer and a detector. The intensity versus wavelength (or energy) plot can then be used to identify the characteristic energy band gap and exciton levels (intrinsic luminescence) of the semiconductor, and the defect energy levels (extrinsic luminescence) within the gap [1].

Both photo- and cathodoluminescence analysis has been performed on AlN, GaN, and $Al_xGa_{1-x}N$ semiconductors [3–8]. Much of the work has been in measuring the low temperature GaN luminescence peaks. Work on AlN has been limited by the energy gap of 6.2 eV, which corresponds to a wavelength (200 nm) that is lower than most of the optical light sources. An excimer laser using the ArF line (193 nm) can be used, but caution must be taken when operating at these wavelengths.

Few time-resolved luminescence measurements have been performed on AlN and GaN. In a time-resolved measurement, a pulsed source is used to excite the sample and the luminescence is measured at short sampling intervals after the pulse. The result is an intensity vs. time plot. Time resolved spectroscopy is useful for separating the emission bands of the investigated samples with different decay times. It is often used to measure donor-acceptor recombination rates and minority carrier lifetimes [1].

Depth-resolved information can be obtained using cathodoluminescence, since generation depth varies with beam voltage. This technique is particularly useful for studying ion implanted semiconductors and layered structures [1].

## B. Future Research Plans and Goals

A combined photo- and cathodoluminescence system has been assembled and will be used to perform luminescence measurements on AlN, GaN, and $Al_xGa_{1-x}N$ semiconductors. A schematic view is shown in Fig. 1, and a block diagram is shown in Fig. 2. The sample is in a UHV chamber, and the monochrometer and collection optics are in a vacuum environment. Each sample is attached to a cryostat from APD cryogenics,

which allows for luminescence measurements at temperatures as low as 4.2 K. The monochrometer is a McPherson model 219 vacuum monochrometer. Its focal length is .5 m, with a wavelength resolution of .02 nm at 313.1 nm. This high resolution will allow for the identification of exciton and defect energy levels. A photon counter from Stanford Research (SR-400) with a Hamamatsu Photomultiplier tube is used to acquire the data, and a software package from Galactic Industries (Spectra-Calc) is used to analyze the results.

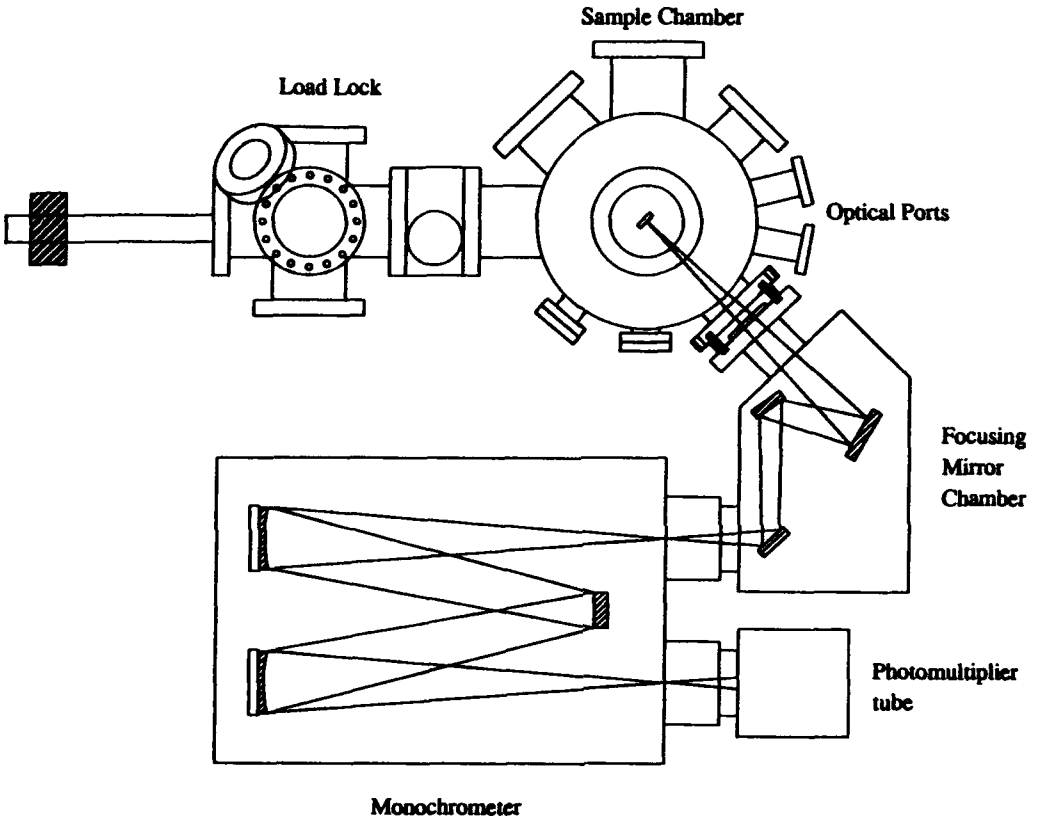


Figure 1. Schematic of the combined photo- and cathodoluminescence system.

Two optical sources and a beam blanking electron gun are the excitation sources. One optical source is a He-Cd laser with a powder of 15 mW. It is a continuous wavelength laser that operates at a wavelength of 325 nm, making it practical for testing the luminescence of GaN. A pulsed excimer laser is the other optical source; it operates at wavelengths of 193 nm (6.4 eV), 248 nm (5.0 eV), and 308 nm (4.0 eV); and so it can be used to measure the luminescence of both AlN and GaN.

The beam blanking capability of the electron gun will allow for time-resolved luminescence measurements of the semiconductors. The SR-400 will be used for data

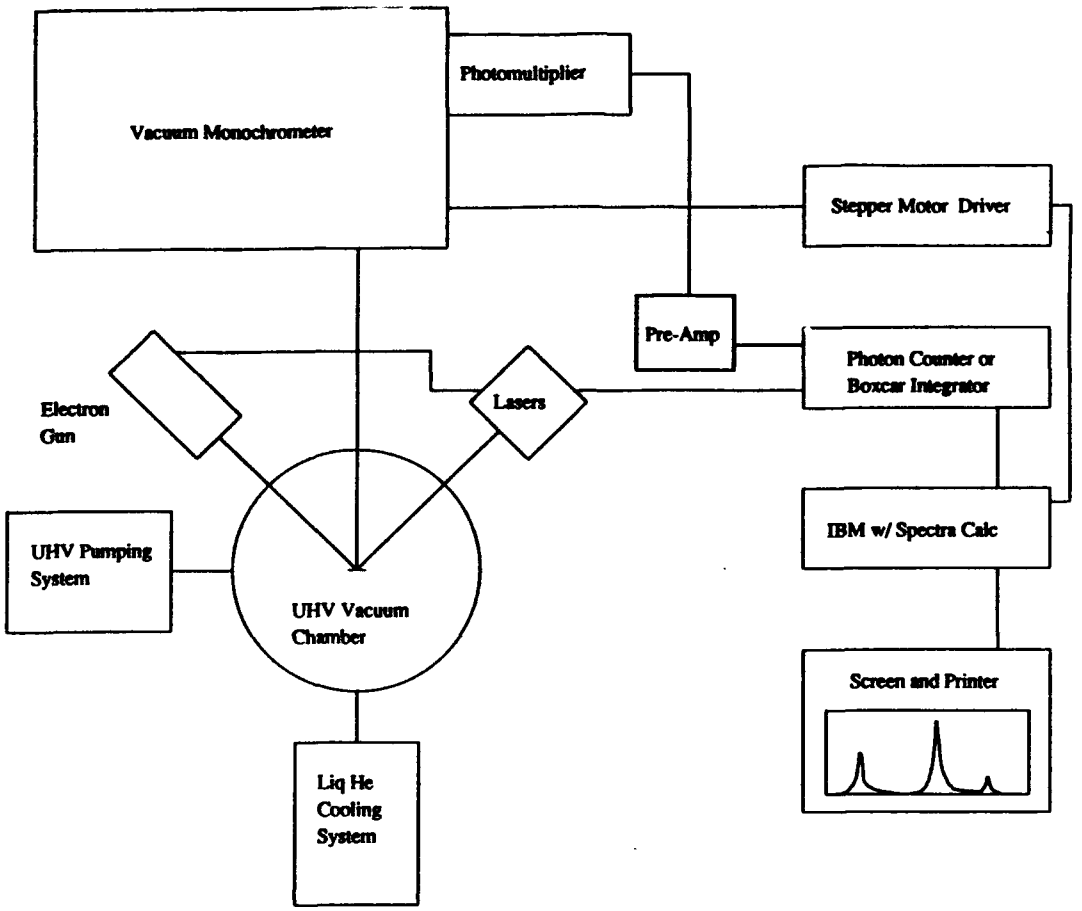


Figure 2. Block diagram of the combined photo- and cathodoluminescence system.

collection, although a boxcar integrator may also be used. The electron gun has a maximum beam voltage of 10 keV, which allows for depth-resolved spectroscopy to be performed.

Cathodoluminescence in the TEM will also be performed on the nitride films through a collaboration with Dr. Roger Graham at Arizona State University. In the TEM environment the luminescence from individual defects can be examined, and hence the source of extrinsic luminescence peaks can be identified.

## C. References


1. B. G. Yacobi and D. B. Holt, *Cathodoluminescence Microscopy of Inorganic Solids*, Plenum Press, New York (1990).
2. Micheal D. Lumb, Ed., *Luminescence Spectroscopy*, Academic Press, New York (1978).
3. S. Strite and H. Morkoç, GaN, AlN, and InN review.
4. R. A. Youngman and J. H. Harris, J. Am. Ceram. Soc., 73 [11] 3238-46 (1990).
5. S. Strite, J. Ruan, Z. Li, N Manning, A. Salvador, H. Chen, D. J. Smith, W. J. Choyke, and H. Morkoç, An investigation of the properties of b-GaN grown on GaAs.

6. M. A. Khan, R. A. Skogman, J. M. Van Hove, S. Krishnankutty, and R. M. Kolbas, Appl. Phys. Lett. **56** (13) 1257-59 (1990).
7. Z. Sitar, M. J. Paisley, J. Ruan, J. W. Choyke, and R. F. Davis.
8. V. F. Veselov, A. V. Dobrynin, G. A. Naida, P. A. Pundur, E. A. Slotsenietse, and E. B. Sokolov, Inorganic Materials, **25** (9) 1250-4 (1989).

## VIII. Distribution List

| | |
|---|---|
| Mr. Max Yoder<br>Office of Naval Research<br>Electronics Division, Code: 1114SS<br>800 N. Quincy Street<br>Arlington, VA 22217-5000 | 3 |
| Administrative Contracting Officer<br>Office Of Naval Research<br>Resident Representative<br>The Ohio State University Research Center<br>1960 Kenny Road<br>Columbus, OH 43210-1063 | 1 |
| Director, Naval Research Laboratory<br>ATTN: Code 2627<br>Washington, DC 20375 | 1 |
| Defense Technical Information Center<br>Bldg. 5, Cameron Station<br>Alexandria, VA 22314 | 2 |
| Washington Headquarters Services<br>ATTN: Dept. Acctg. Division<br>Room 3B269, The Pentagon<br>Washington, DC 20301-1135 | 2 |